

Light nuclei production via an analytical coalescence model in relativistic heavy ion collisions

王瑞芹 曲阜师范大学

Collaborators: Feng-lan Shao, Jun Song, Yan-ting Feng, et al.

References: Phys. Rev. C **109**, 034907, 2024; **105**, 054908, 2022; **103**, 064908, 2021.

Outline

I. Introduction

II. Analytical coalescence model

the general formalism

delta function approximation

modeling the normalized nucleon coordinate distribution

final formulas of momentum distributions of light nuclei

III. Applications at RHIC and LHC

B_A in pp, p-Pb and Pb-Pb collisions at LHC

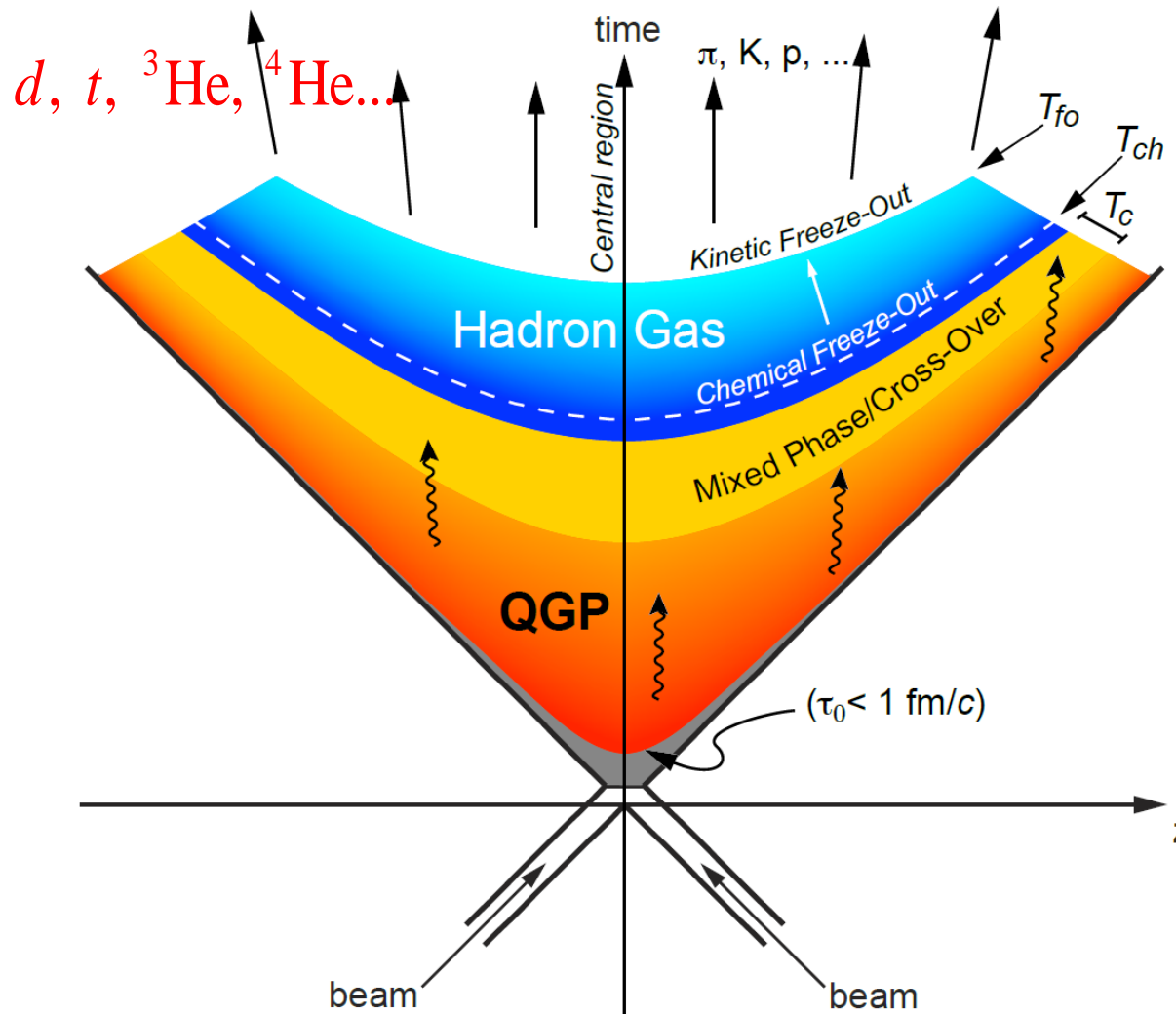
p_T spectra, yield rapidity densities, yield ratios at RHIC and LHC

extended applications in Au-Au collisions at 3 GeV

IV. Summary

I. Introduction

What can **light nuclei** in relativistic heavy-ion collisions tell us?



- composite particle production mechanism
- system freeze-out property
- QCD phase diagram structure
-

Theoretical studies

thermal models

$$N_i = V \int \frac{d^3 p}{(2\pi)^3} \frac{g_i}{\exp[(\sqrt{p^2 + m_i^2} - \mu_i)/T_{ch}] \pm 1},$$

coalescence models

$$f_{LN} \sim f_p^Z f_n^{A-Z} \otimes R_{LN}$$

dynamical transport models

$$\pi d \leftrightarrow \pi pn; \pi t \leftrightarrow \pi pnn; \pi^3\text{He} \leftrightarrow \pi ppn; Nd \leftrightarrow Npn; \dots$$

multi-fragmentation

break-up of highly excited spectators

Experimental measurements

- p_T spectra
- rapidity distributions
- yield ratios
- coalescence factors B_2 and B_3
- flows v_1, v_2 and v_3
-

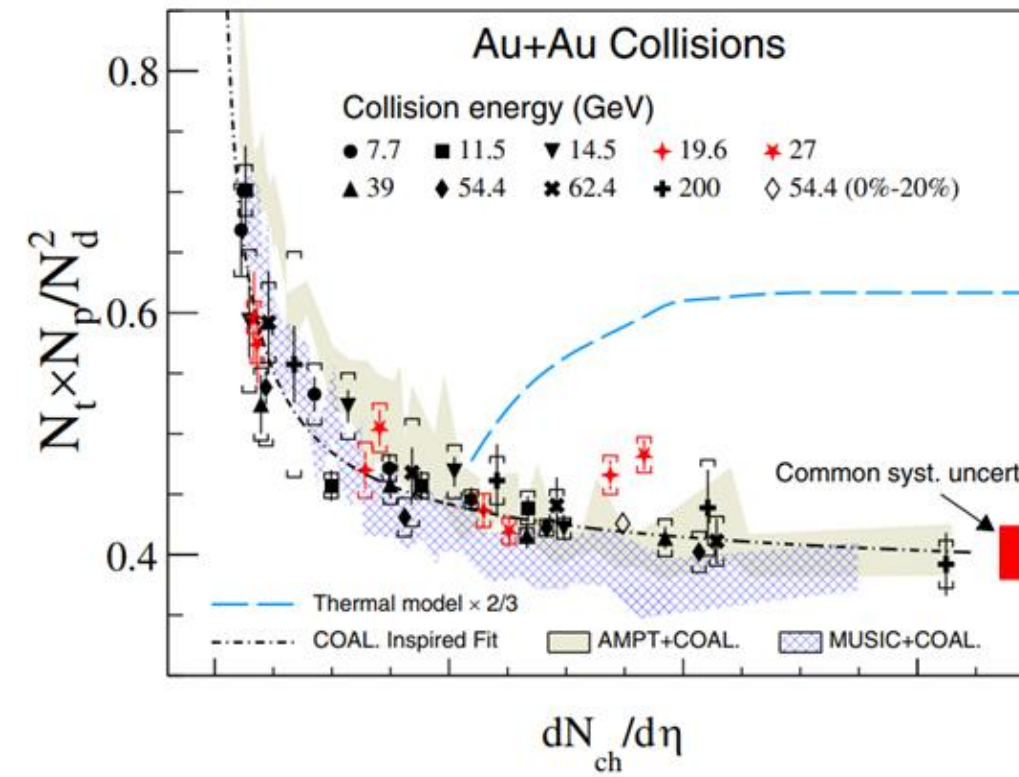
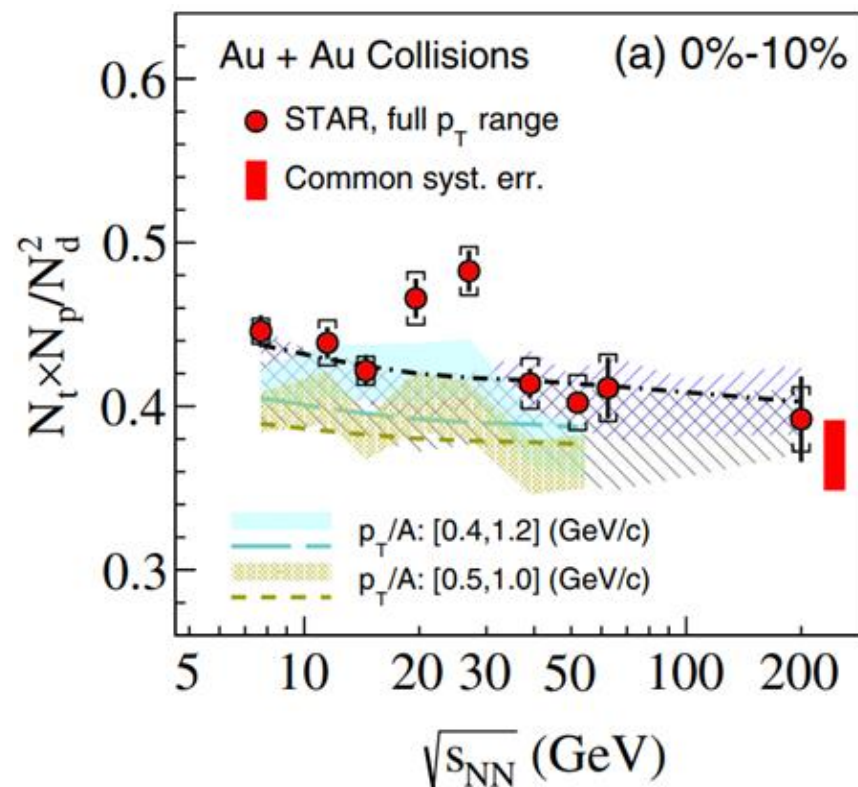
collision energy dependence

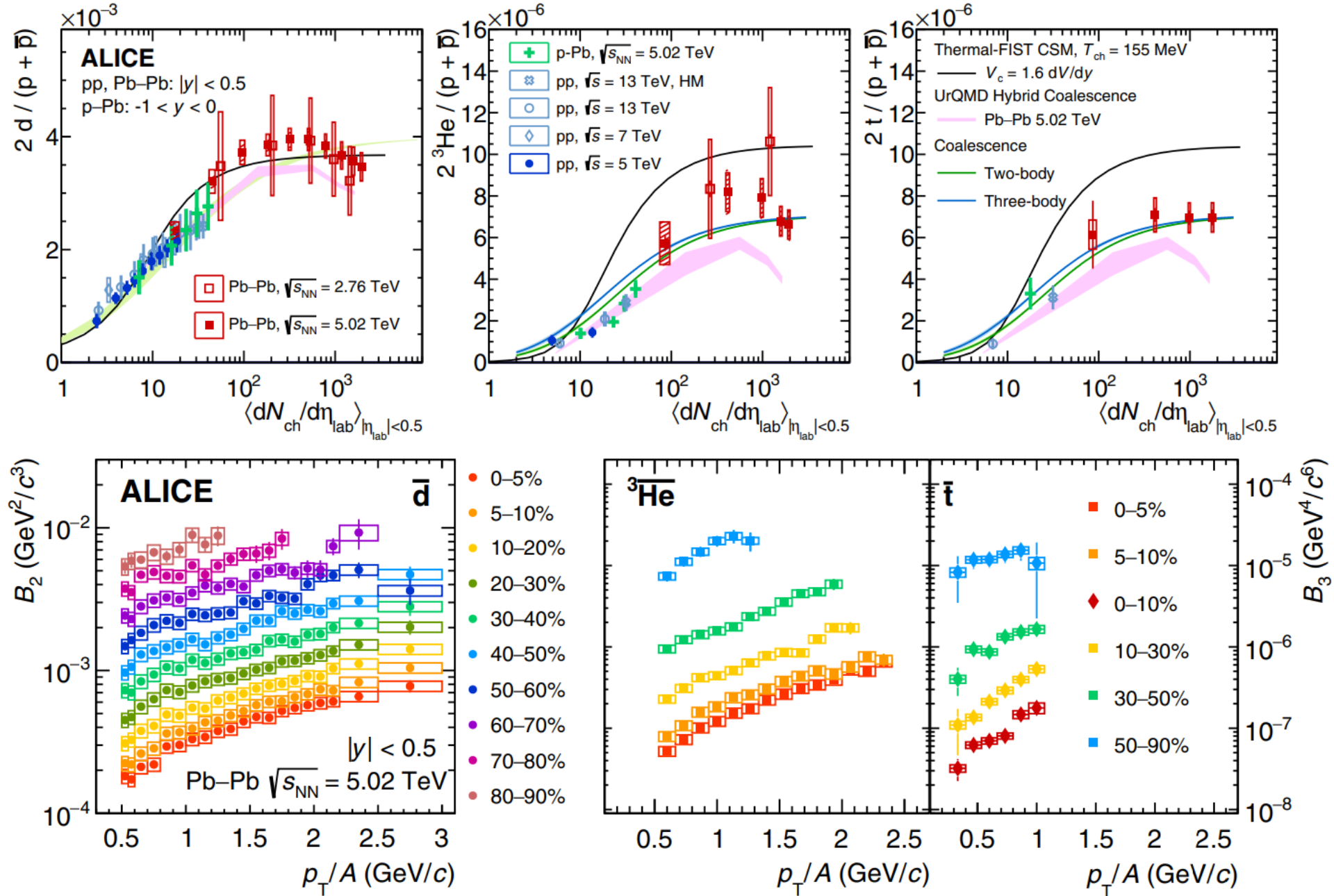
system size dependence

p_T dependence

RHIC Experiment:

STAR, PRL 130, 202301, 2023





How **coalescence** works for those RHIC & LHC measurements ?

Characteristics originated from **coalescence** itself ?

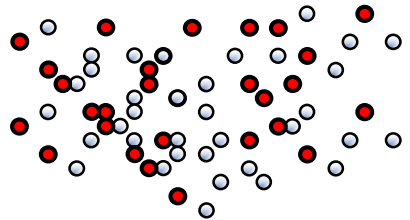


We develop an analytic description for the productions of different species of light nuclei in the coalescence picture --
- the analytical coalescence model.

How **milk** works for these delicious foods ?

II. Analytical coalescence model

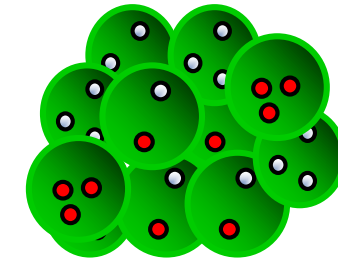
quark-antiquark system



$$q = u, d, s, c, b$$

$$\bar{q} = \bar{u}, \bar{d}, \bar{s}, \bar{c}, \bar{b}$$

hadronic system



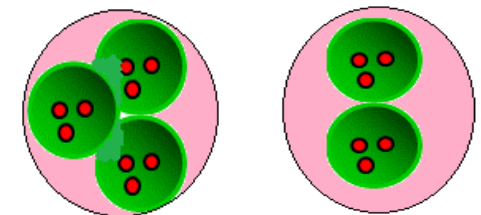
combination →

**Shandong Quark
Combination Model**

$$M(q\bar{q}), B(qqq), \overline{B}(\overline{q}\overline{q})$$

re-combination

Nucleon Coalescence Model



$$d, t, {}^3\text{He}, {}^3\text{H}, {}^4\text{He}...$$

$$p + n \rightarrow d$$

The deuteron momentum distribution

$$f_d(\vec{p}) = \int d\vec{x}_1 d\vec{x}_2 d\vec{p}_1 d\vec{p}_2 f_{pn}(\vec{x}_1, \vec{x}_2; \vec{p}_1, \vec{p}_2) \mathcal{R}_d(\vec{x}_1, \vec{x}_2; \vec{p}_1, \vec{p}_2, \vec{p})$$

two-nucleon joint coordinate momentum distribution

$$f_{pn}(\vec{x}_1, \vec{x}_2; \vec{p}_1, \vec{p}_2) = N_{pn} f_{pn}^{(n)}(\vec{x}_1, \vec{x}_2; \vec{p}_1, \vec{p}_2)$$

kernel function $\mathcal{R}_d(\vec{x}_1, \vec{x}_2; \vec{p}_1, \vec{p}_2, \vec{p}) = g_d \mathcal{R}_d^{(x,p)}(\vec{x}_1, \vec{x}_2; \vec{p}_1, \vec{p}_2) \delta(\sum_{i=1}^2 \vec{p}_i - \vec{p})$

$$\mathcal{R}_d^{(x,p)}(\vec{x}_1, \vec{x}_2; \vec{p}_1, \vec{p}_2) = 8e^{-\frac{(\vec{x}'_1 - \vec{x}'_2)^2}{\sigma_d^2}} e^{-\frac{\sigma_d^2 (\vec{p}'_1 - \vec{p}'_2)^2}{4\hbar^2 c^2}}, \quad \sigma_d = \sqrt{\frac{8}{3}} R_d$$

The deuteron momentum distribution

$$f_d(\vec{p}) = g_d N_{pn} \int d\vec{x}_1 d\vec{x}_2 d\vec{p}_1 d\vec{p}_2 f_{pn}^{(n)}(\vec{x}_1, \vec{x}_2; \vec{p}_1, \vec{p}_2) 8e^{-\frac{(\vec{x}'_1 - \vec{x}'_2)^2}{\sigma_d^2}} e^{-\frac{\sigma_d^2 (\vec{p}'_1 - \vec{p}'_2)^2}{4\hbar^2 c^2}} \delta(\sum_{i=1}^2 \vec{p}_i - \vec{p})$$

Assumption 1: delta function approximation

$$e^{-\frac{\sigma_d^2 (\vec{p}'_1 - \vec{p}'_2)^2}{4\hbar^2 c^2}} \approx \left(\frac{2\hbar c \sqrt{\pi}}{\sigma_d}\right)^3 \delta(\vec{p}'_1 - \vec{p}'_2)$$

We have $f_d(\vec{p}) = 8g_d N_{pn} \left(\frac{\hbar c \sqrt{\pi}}{\sigma_d}\right)^3 \gamma \int d\vec{x}_1 d\vec{x}_2 f_{pn}^{(n)}(\vec{x}_1, \vec{x}_2; \frac{\vec{p}}{2}, \frac{\vec{p}}{2}) e^{-\frac{(\vec{x}'_1 - \vec{x}'_2)^2}{\sigma_d^2}}$

Assumption 2: $f_{pn}^{(n)}(\vec{x}_1, \vec{x}_2; \frac{\vec{p}}{2}, \frac{\vec{p}}{2}) = f_{pn}^{(n)}(\vec{X}) f_{pn}^{(n)}(\vec{r}; \frac{\vec{p}}{2}, \frac{\vec{p}}{2})$

$$\vec{X} = \frac{\vec{x}_1 + \vec{x}_2}{2}$$

$$\vec{r} = \vec{x}_1 - \vec{x}_2$$

The deuteron momentum distribution

$$f_d(\vec{p}) = 8g_d N_{pn} \left(\frac{\hbar c \sqrt{\pi}}{\sigma_d} \right)^3 \gamma \int d\vec{r} f_{pn}^{(n)}(\vec{r}; \frac{\vec{p}}{2}, \frac{\vec{p}}{2}) e^{-\frac{(\vec{r}')^2}{\sigma_d^2}}$$

adopting $f_{pn}^{(n)}(\vec{r}; \frac{\vec{p}}{2}, \frac{\vec{p}}{2}) = \frac{1}{[\pi CR_f^2(\vec{p})]^{3/2}} e^{-\frac{\vec{r}^2}{CR_f^2(\vec{p})}} f_{pn}(\frac{\vec{p}}{2}, \frac{\vec{p}}{2})$

We finally have

$$f_d(\vec{p}) = \frac{8g_d (\hbar c \sqrt{\pi})^3 \gamma}{[CR_f^2(\vec{p}) + \sigma_d^2] \sqrt{C[R_f(\vec{p})/\gamma]^2 + \sigma_d^2}} f_{pn}(\frac{\vec{p}}{2}, \frac{\vec{p}}{2})$$

$$f_d^{(\text{inv})}(p_T) = \frac{32(\hbar c \sqrt{\pi})^3 g_d}{m_d [CR_f^2(p_T) + \sigma_d^2] \sqrt{C[R_f(p_T)/\gamma]^2 + \sigma_d^2}} f_p^{(\text{inv})}(\frac{p_T}{2}) f_n^{(\text{inv})}(\frac{p_T}{2})$$

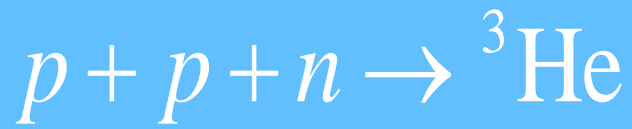


$$p + n + n \rightarrow t$$

Three dimensional momentum distribution

$$f_t(\vec{p}) = \frac{8^2 (\hbar^2 c^2 \pi)^3 g_t \gamma^2}{3\sqrt{3} \left[\frac{C}{2} R_f^2(\vec{p}) + \sigma_t^2 \right] \sqrt{\frac{C}{2} [R_f(\vec{p})/\gamma]^2 + \sigma_t^2} \left[\frac{2C}{3} R_f^2(\vec{p}) + \sigma_t^2 \right] \sqrt{\frac{2C}{3} [R_f(\vec{p})/\gamma]^2 + \sigma_t^2}} f_{pnn}\left(\frac{\vec{p}}{3}, \frac{\vec{p}}{3}, \frac{\vec{p}}{3}\right)$$

$$f_t^{(\text{inv})}(p_T) = \frac{192\sqrt{3}(\hbar^2 c^2 \pi)^3 g_t}{m_t^2 \left[\frac{C}{2} R_f^2(p_T) + \sigma_t^2 \right] \sqrt{\frac{C}{2} [R_f(p_T)/\gamma]^2 + \sigma_t^2} \left[\frac{2C}{3} R_f^2(p_T) + \sigma_t^2 \right] \sqrt{\frac{2C}{3} [R_f(p_T)/\gamma]^2 + \sigma_t^2}} \\ \times f_p^{(\text{inv})}\left(\frac{p_T}{3}\right) f_n^{(\text{inv})}\left(\frac{p_T}{3}\right) f_n^{(\text{inv})}\left(\frac{p_T}{3}\right)$$



Three dimensional momentum distribution

$$f_{{}^3\text{He}}(\vec{p}) = \frac{8^2 (\hbar^2 c^2 \pi)^3 g_{{}^3\text{He}} \gamma^2}{3\sqrt{3} \left[\frac{C}{2} R_f^2(\vec{p}) + \sigma_{{}^3\text{He}}^2 \right] \sqrt{\frac{C}{2} [R_f(\vec{p})/\gamma]^2 + \sigma_{{}^3\text{He}}^2} \left[\frac{2C}{3} R_f^2(\vec{p}) + \sigma_{{}^3\text{He}}^2 \right] \sqrt{\frac{2C}{3} [R_f(\vec{p})/\gamma]^2 + \sigma_{{}^3\text{He}}^2}} f_{ppn}\left(\frac{\vec{p}}{3}, \frac{\vec{p}}{3}, \frac{\vec{p}}{3}\right)$$

$$f_{{}^3\text{He}}^{(\text{inv})}(p_T) = \frac{192\sqrt{3}(\hbar^2 c^2 \pi)^3 g_{{}^3\text{He}}}{m_{{}^3\text{He}}^2 \left[\frac{C}{2} R_f^2(p_T) + \sigma_{{}^3\text{He}}^2 \right] \sqrt{\frac{C}{2} [R_f(p_T)/\gamma]^2 + \sigma_{{}^3\text{He}}^2} \left[\frac{2C}{3} R_f^2(p_T) + \sigma_{{}^3\text{He}}^2 \right] \sqrt{\frac{2C}{3} [R_f(p_T)/\gamma]^2 + \sigma_{{}^3\text{He}}^2}} \\ \times f_p^{(\text{inv})}\left(\frac{p_T}{3}\right) f_p^{(\text{inv})}\left(\frac{p_T}{3}\right) f_n^{(\text{inv})}\left(\frac{p_T}{3}\right)$$

$$R_f(p_T) = \color{magenta}{a} \times \color{blue}{\left(\frac{dN_{ch}}{d\eta} \right)^{1/3}} \times \left(\sqrt{p_T^2 + m_{d,t,{}^3\text{He}}^2} \right)^{\color{magenta}{b}} \quad \text{model parameters: } \color{magenta}{a}, \color{magenta}{b}$$

III. Applications at RHIC and LHC

- B_A (B_2, B_3)

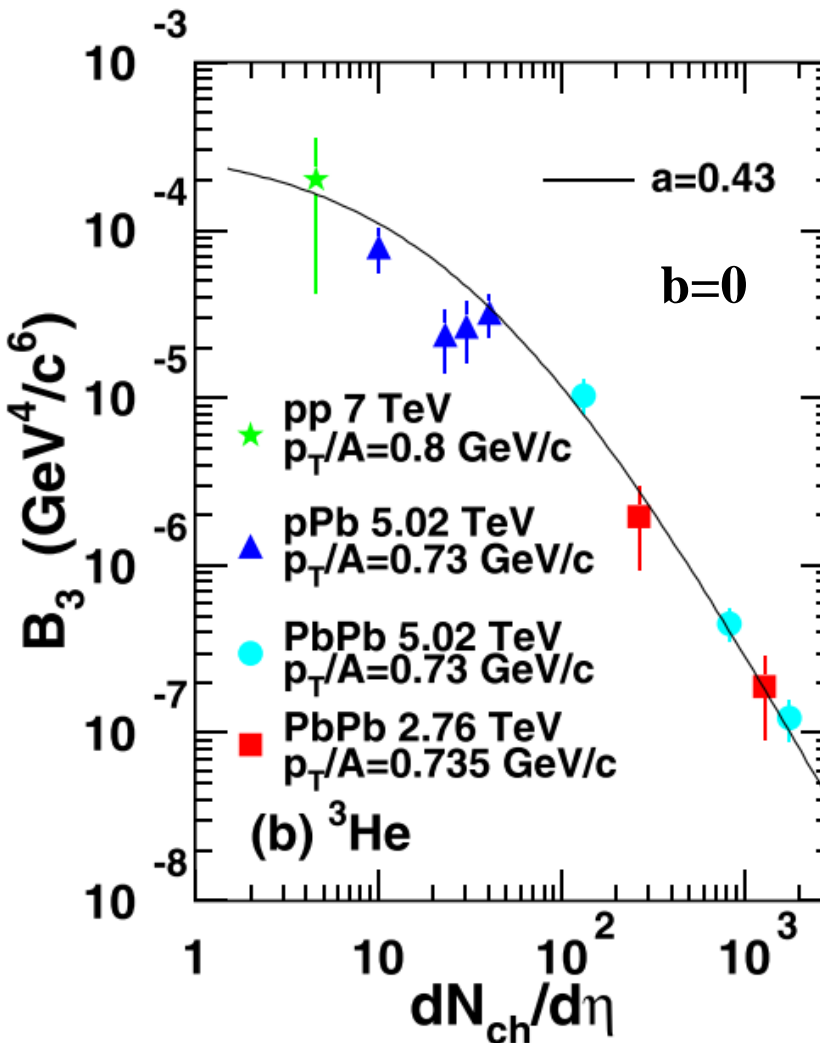
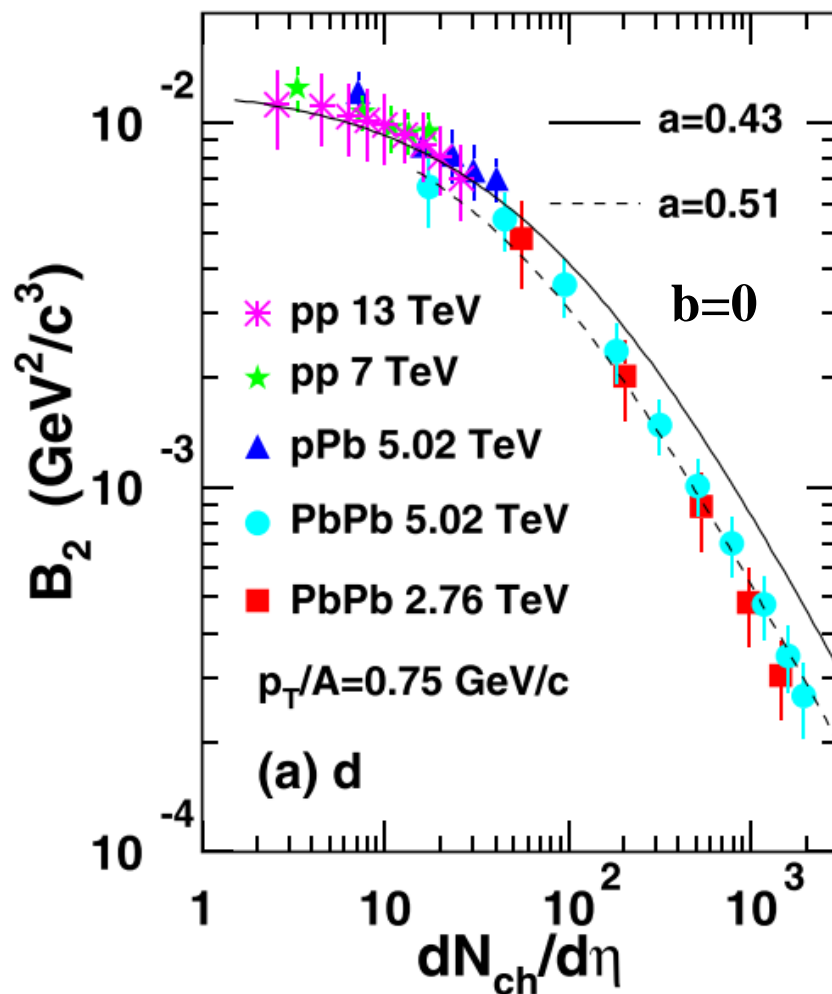
independent of primordial nucleon momentum distributions

- p_T spectra, $\langle p_T \rangle$, yield rapidity densities, ratios...

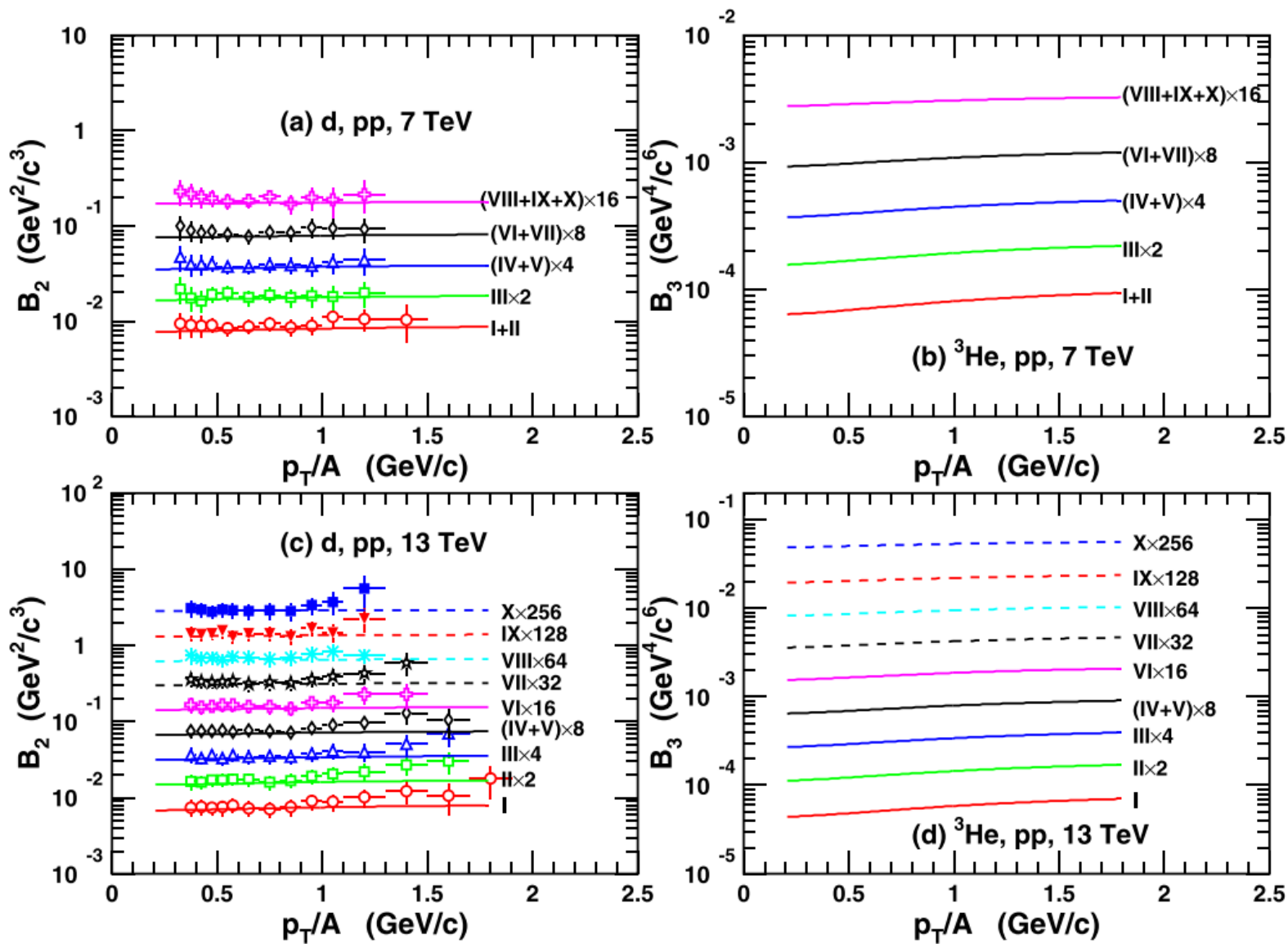
need primordial nucleon momentum distributions as inputs

B_A at $p_T/A=0.7$ GeV/c in pp, p-Pb, Pb-Pb collisions at LHC

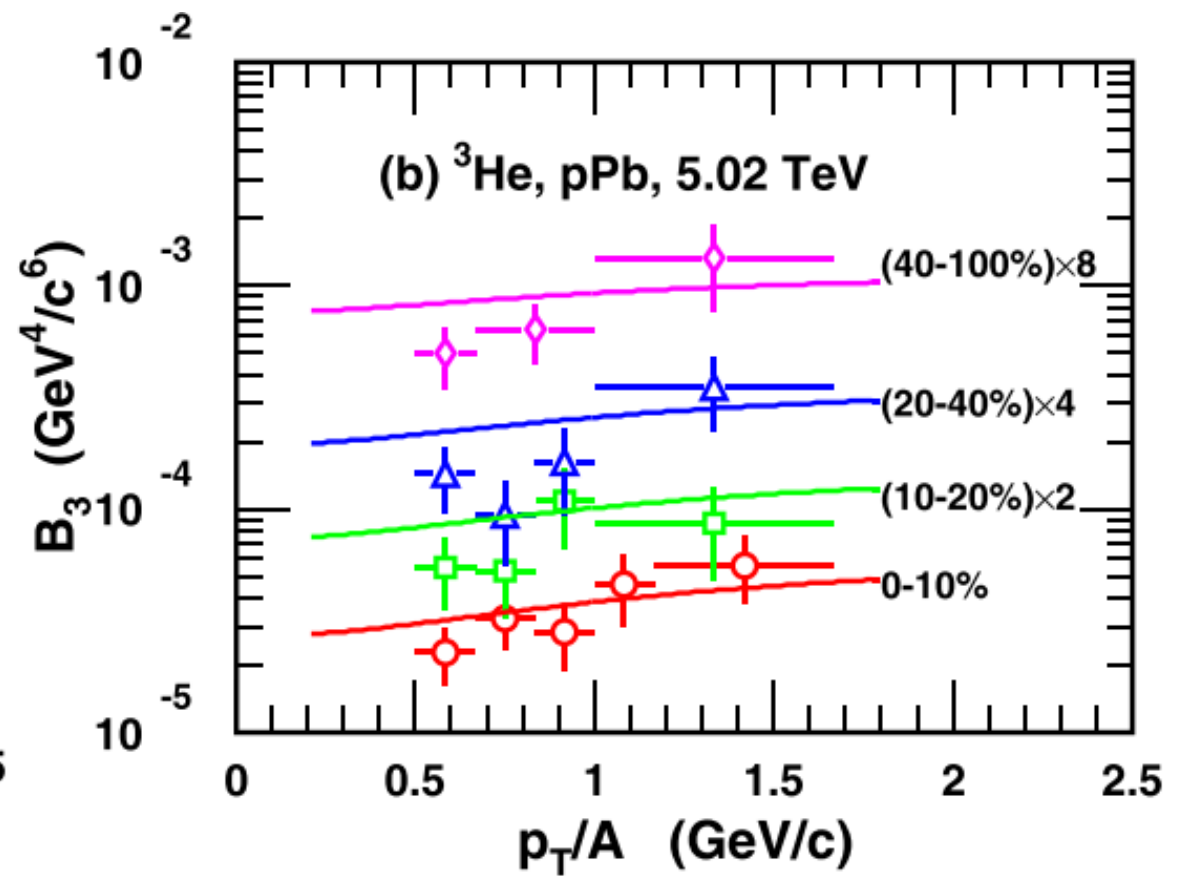
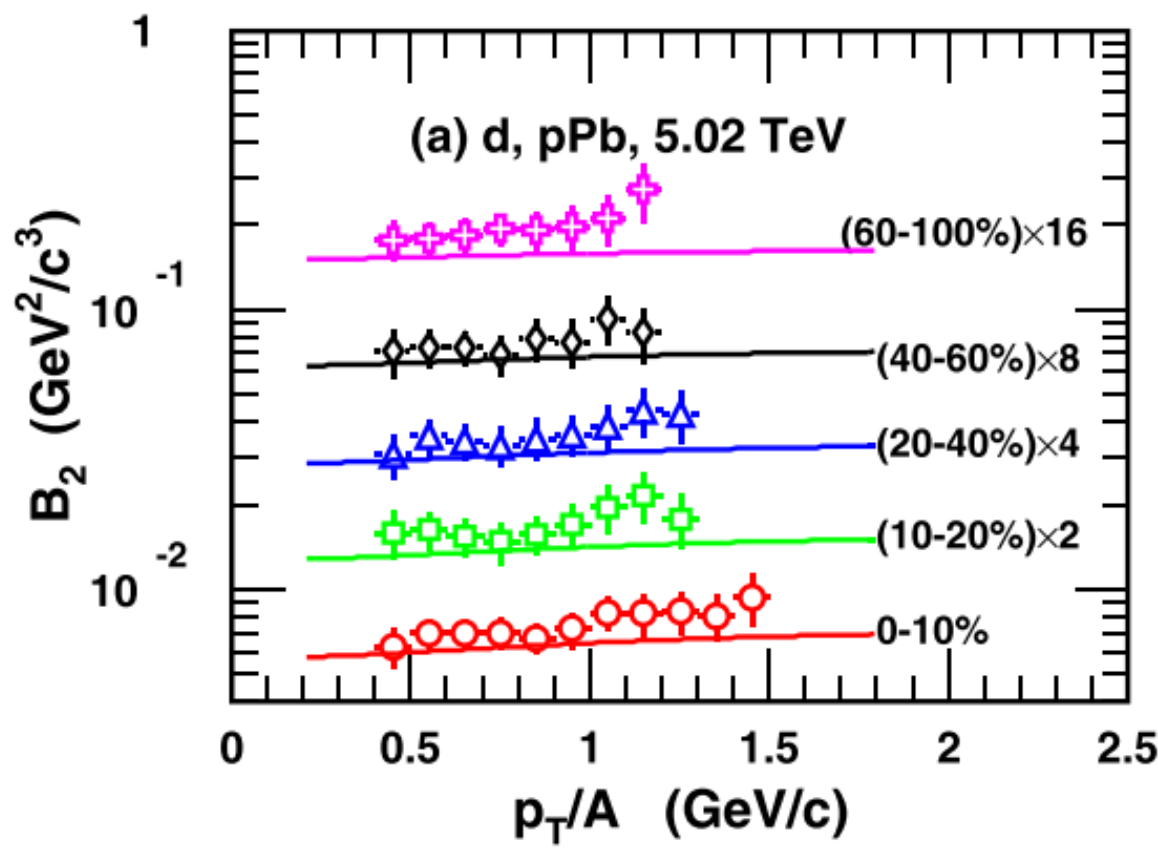
RQW, F.L. Shao, J. Song, PRC 103, 064908, 2021



B_A as function of p_T/A in pp collisions at LHC

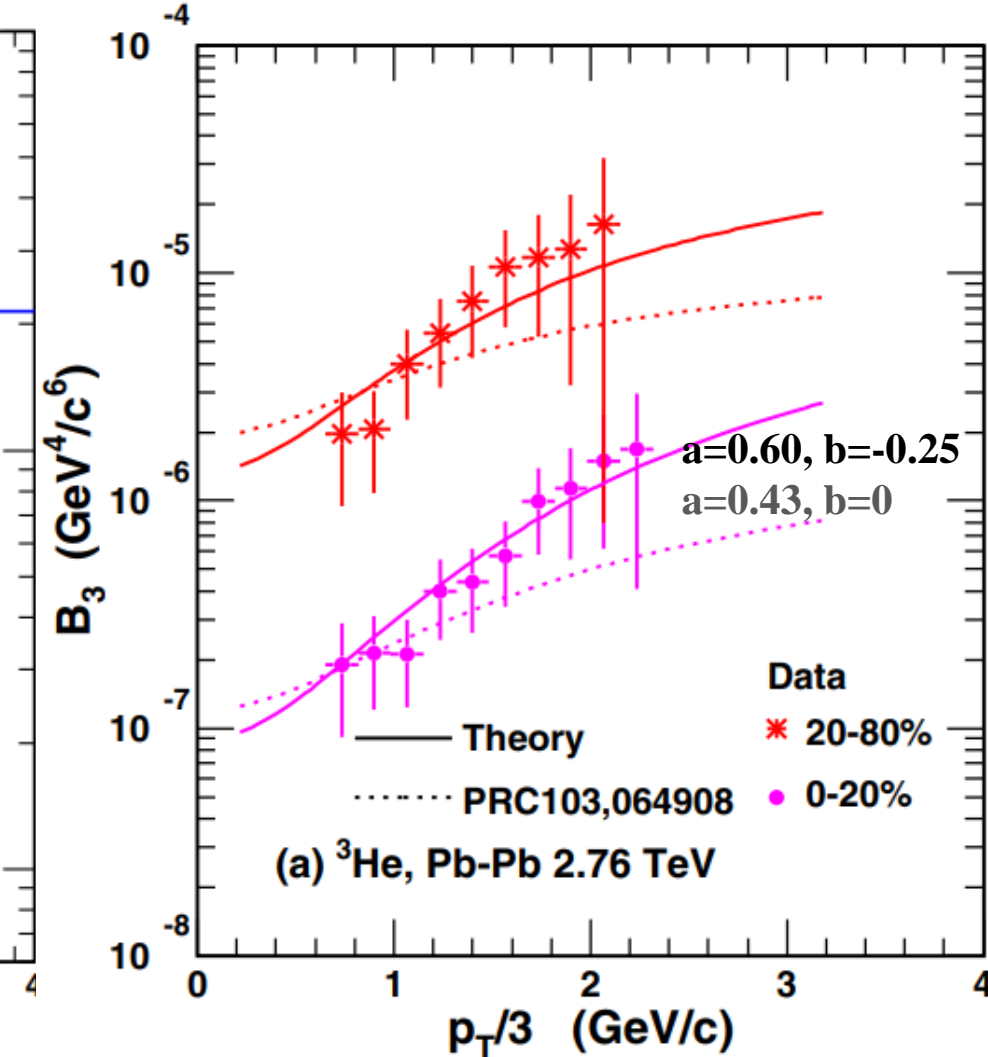
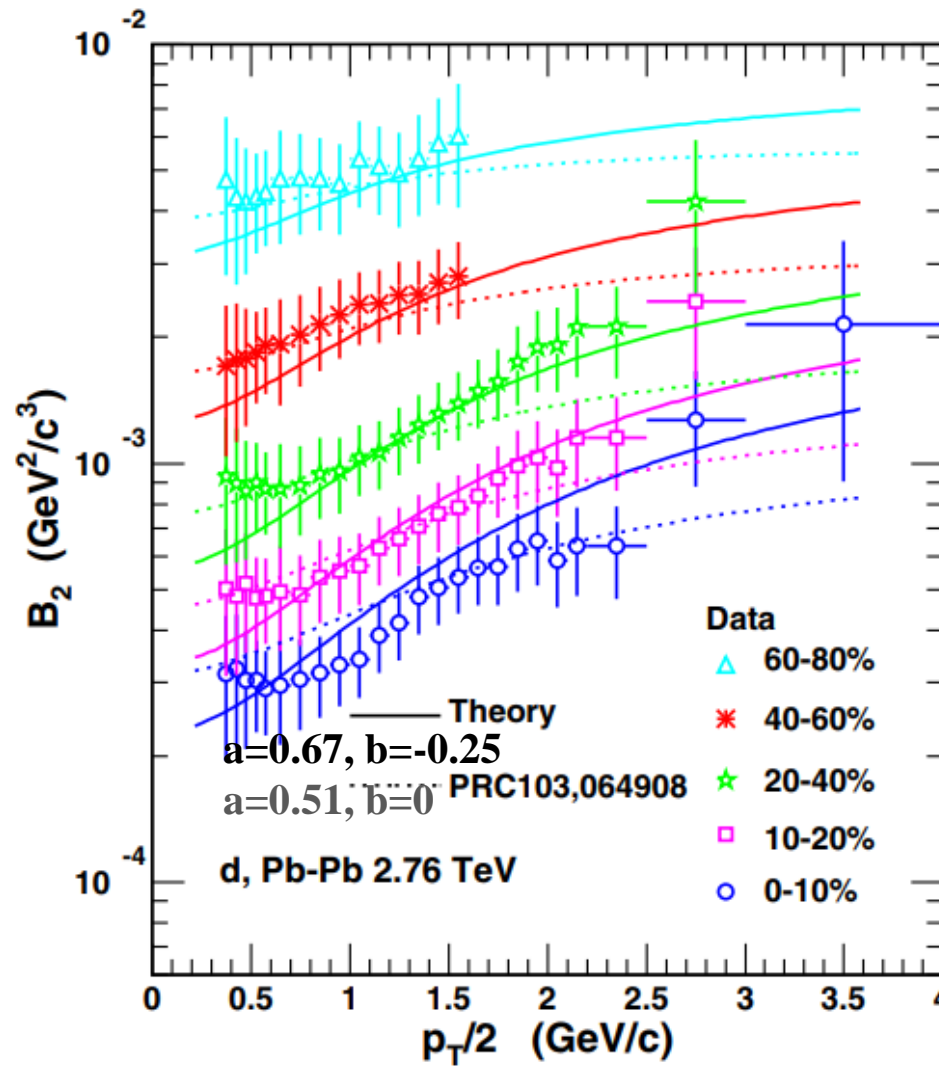


B_A as function of p_T/A in p-Pb collisions at LHC



B_A as function of p_T/A in Pb-Pb collisions at LHC

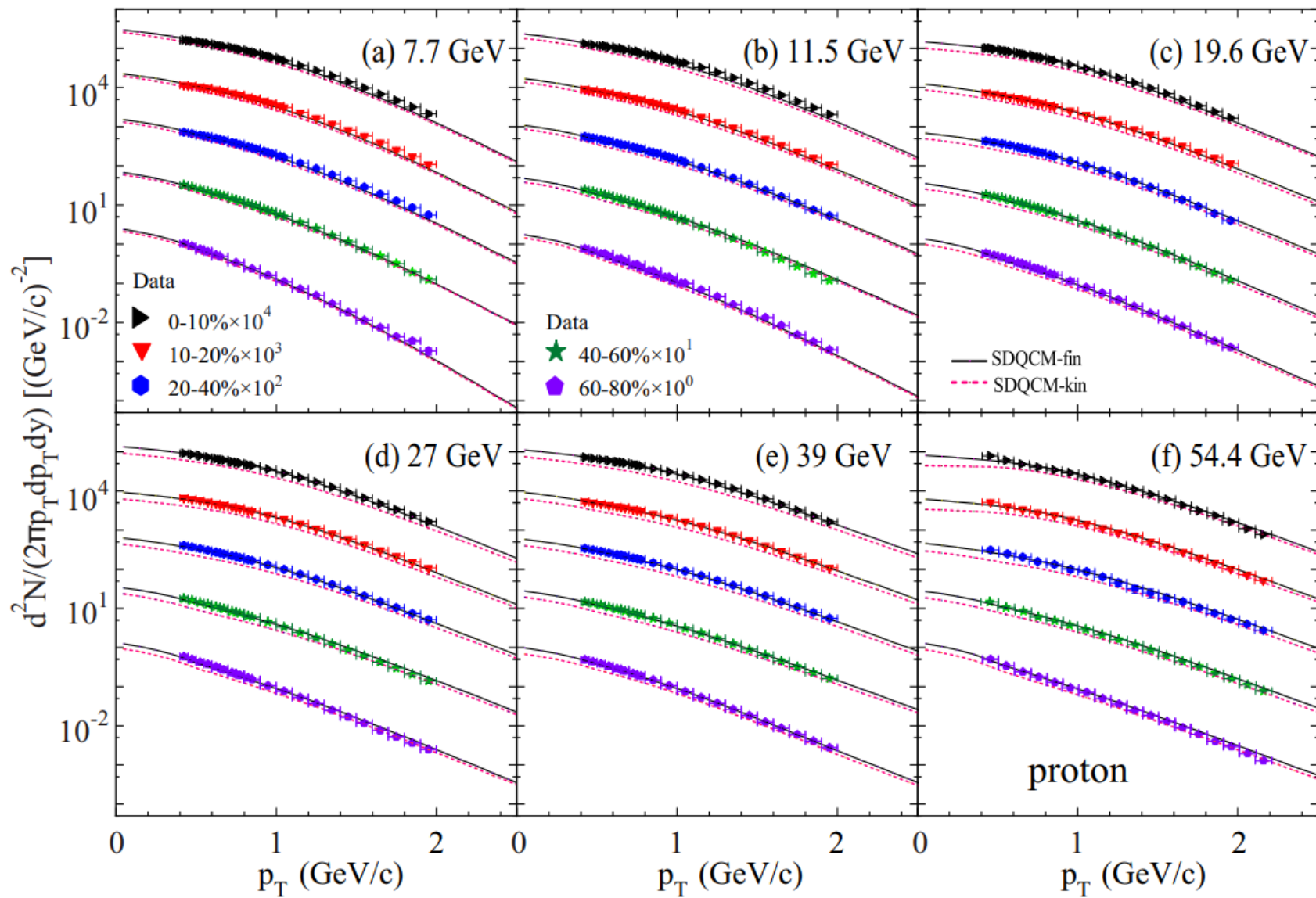
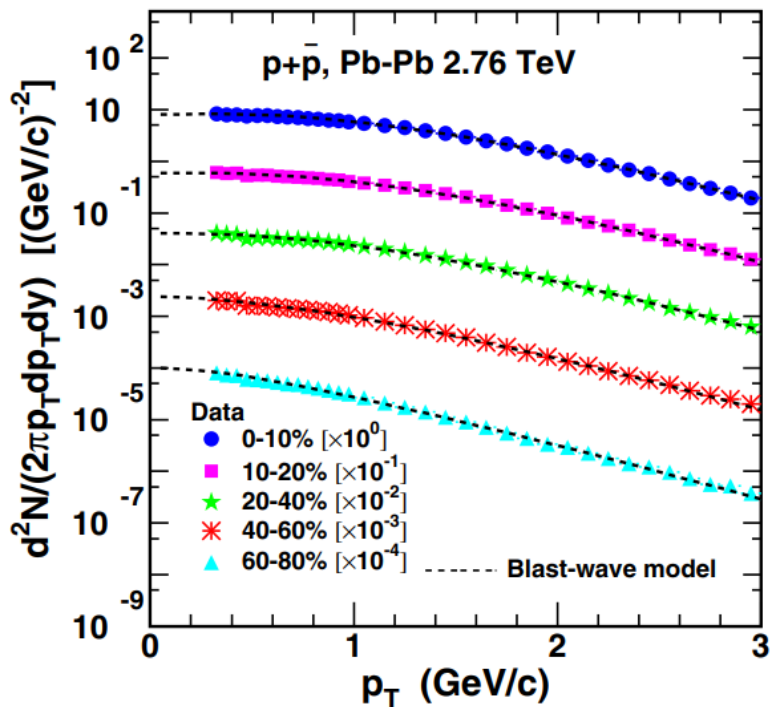
RQW, Y.H. Li, J. Song, F.L. Shao, PRC 109, 034907, 2024



From results of B_A , we find:

- **Analytical coalescence model can give obvious growth of B_A against p_T in Pb-Pb collisions but relatively weak p_T dependence in pp and p-Pb collisions.**
- **Coordinate-momentum correlation is necessary in large Pb-Pb collisions.**

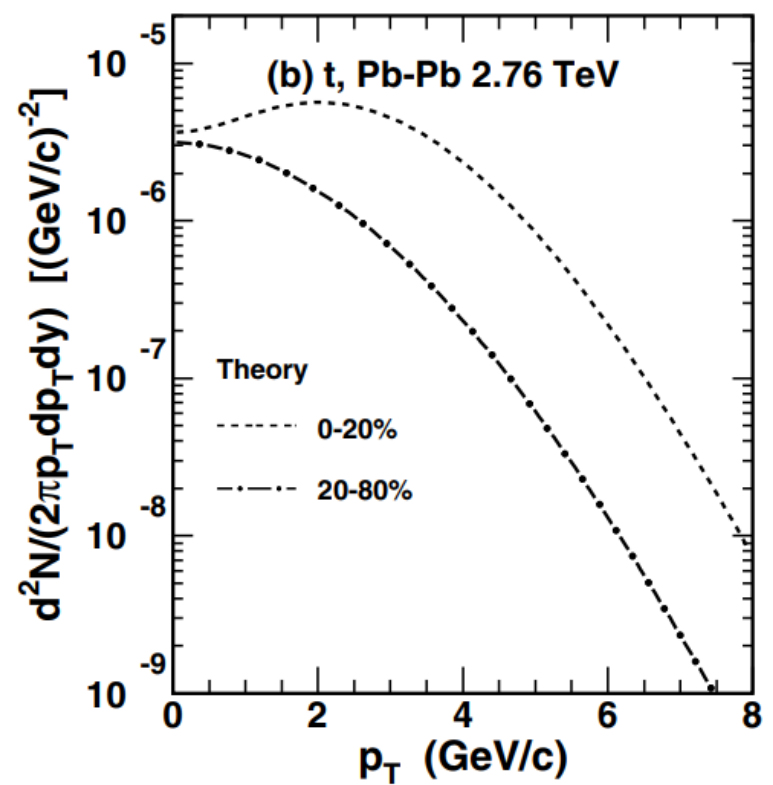
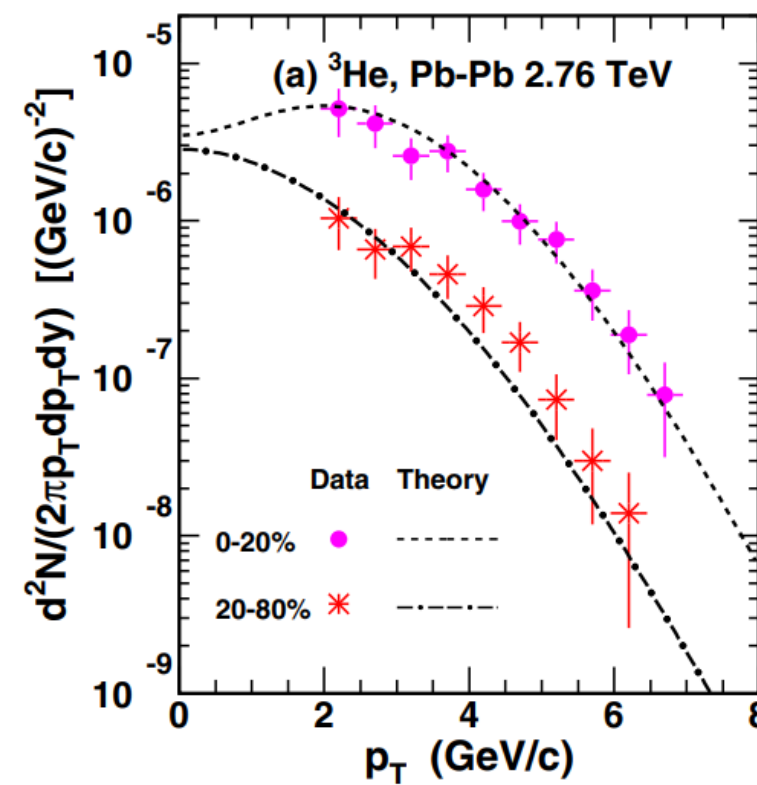
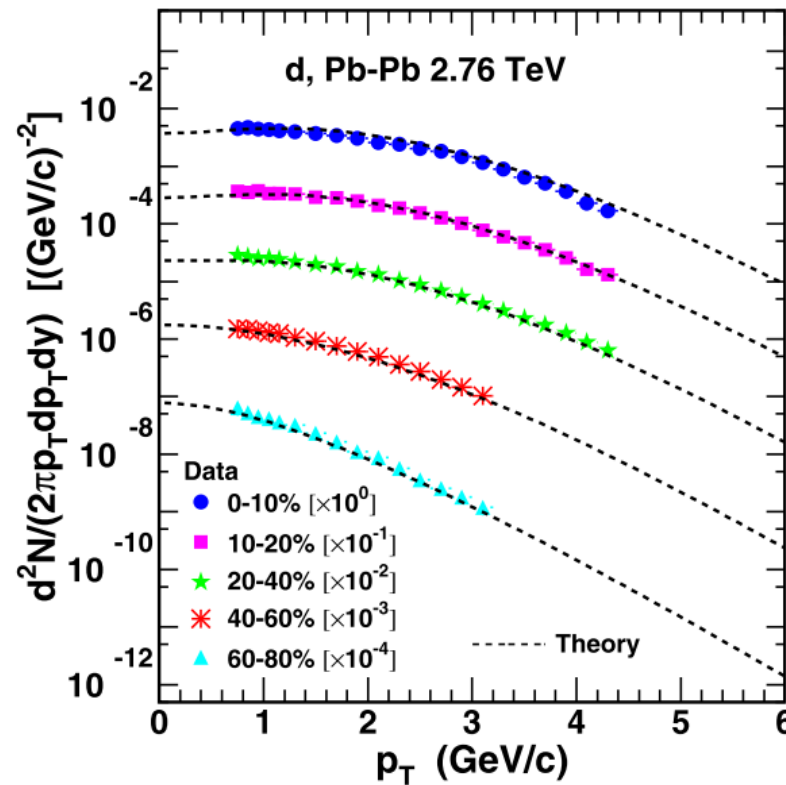
p_T spectra, $\langle p_T \rangle$, yield rapidity densities, ratios



Inputs: proton distributions

Results at LHC

RQW, Y.H. Li, J. Song, F.L. Shao, Phys. Rev. C 109, 034907, 2024



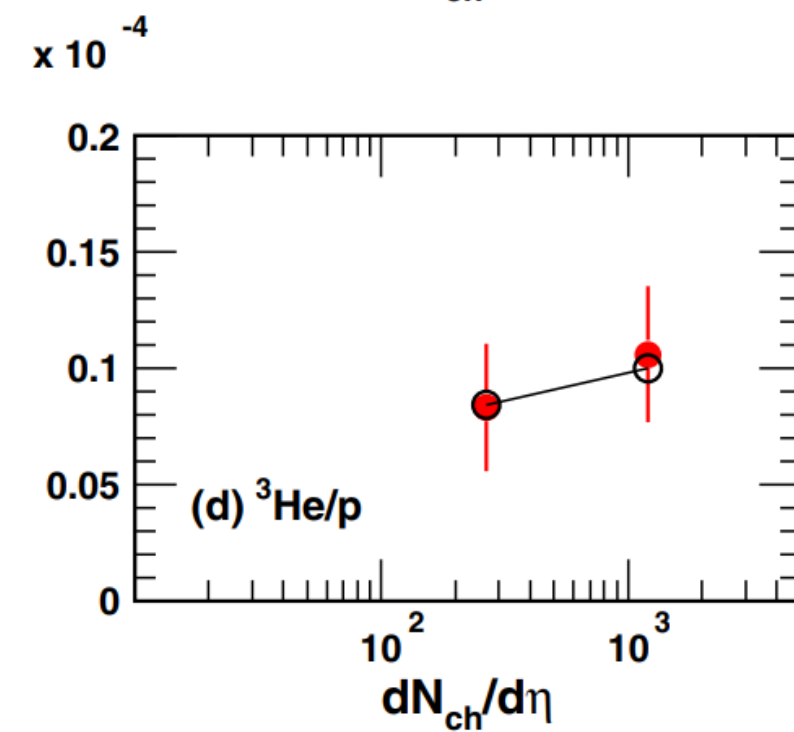
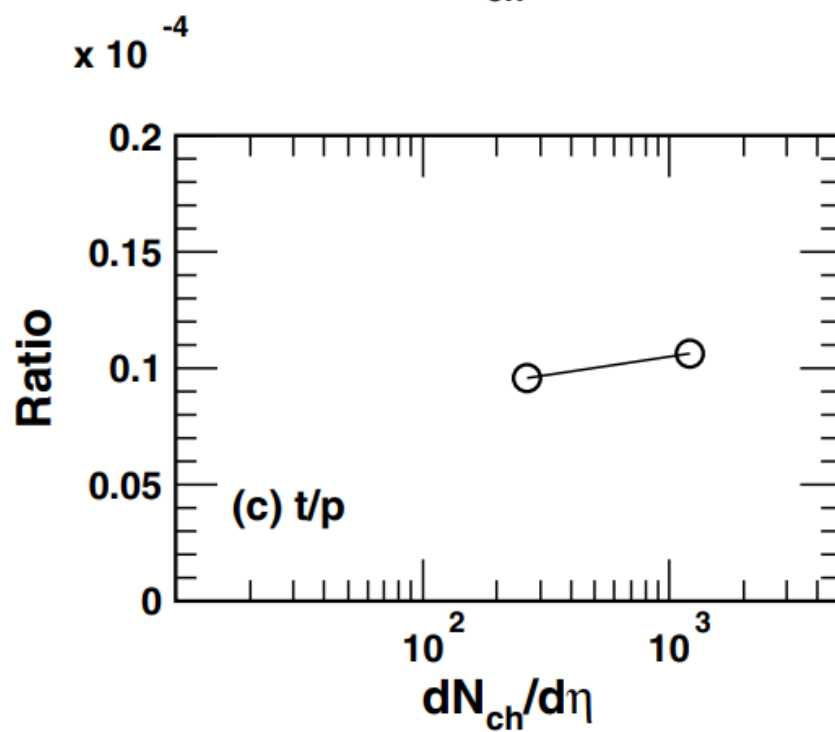
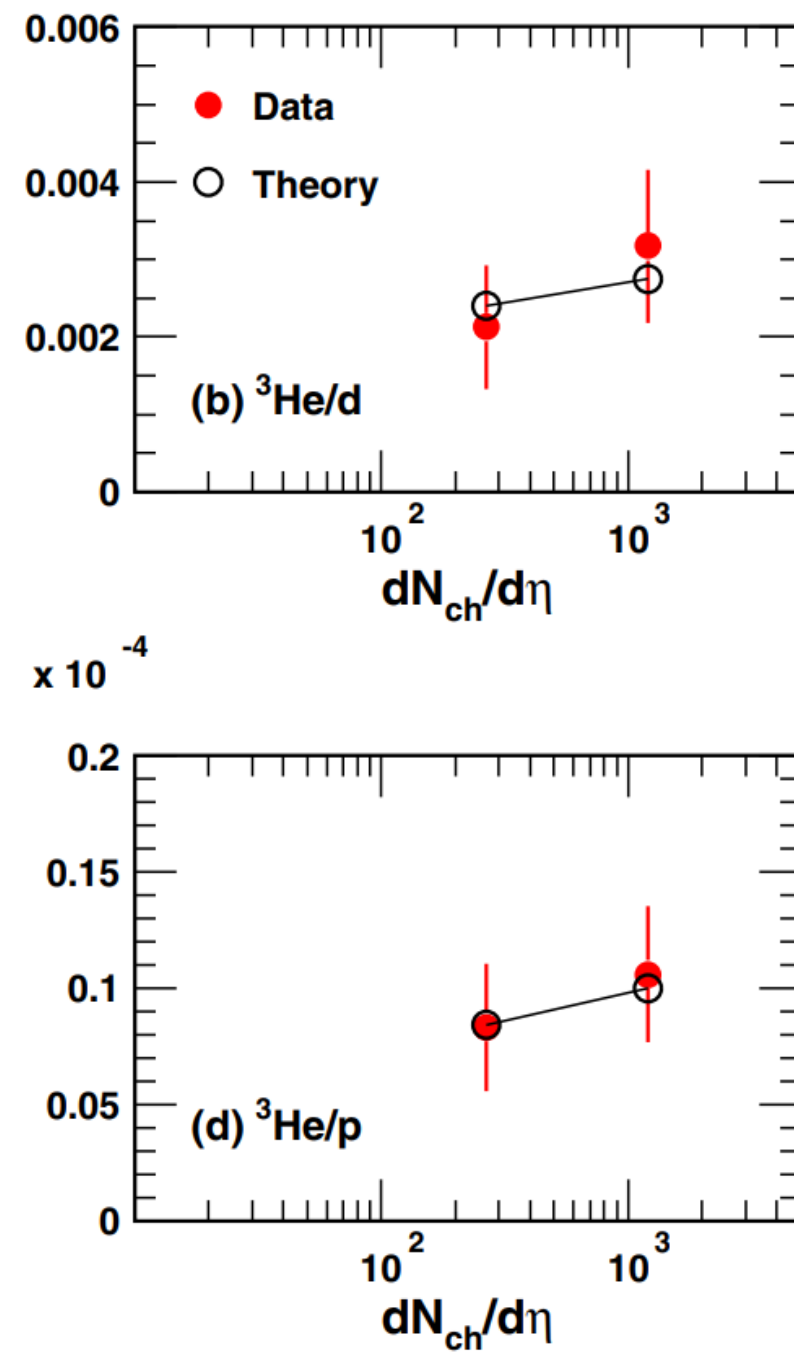
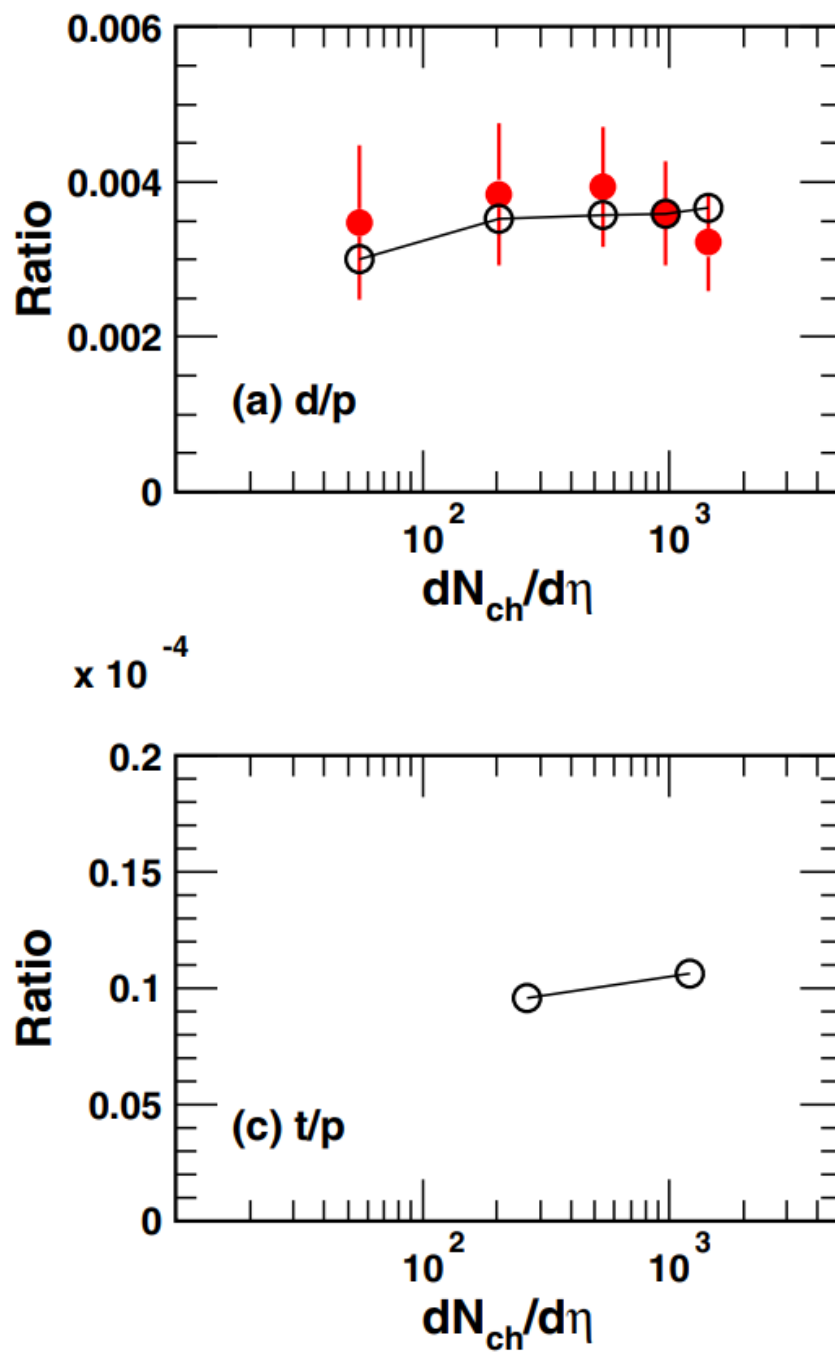
p_T spectra of d, ${}^3\text{He}$, t

$\langle p_T \rangle$ and dN/dy in Pb-Pb 2.76 TeV

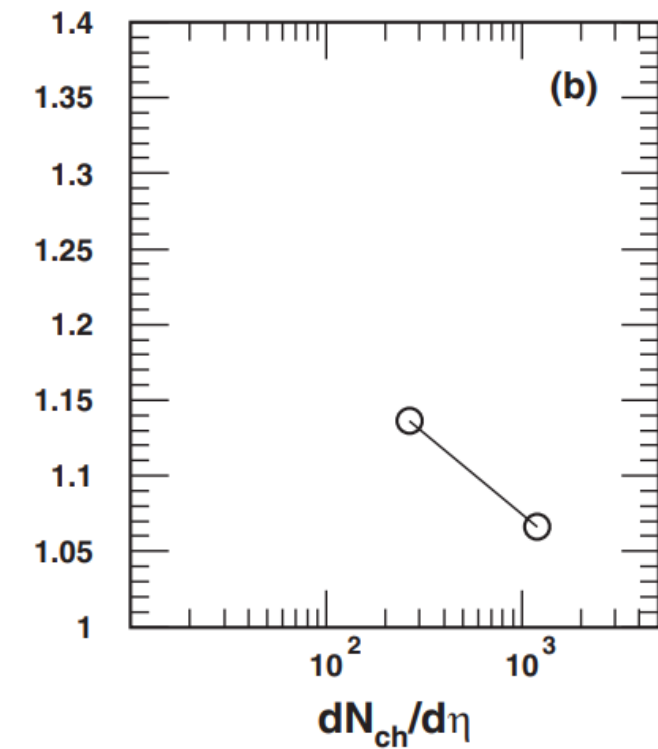
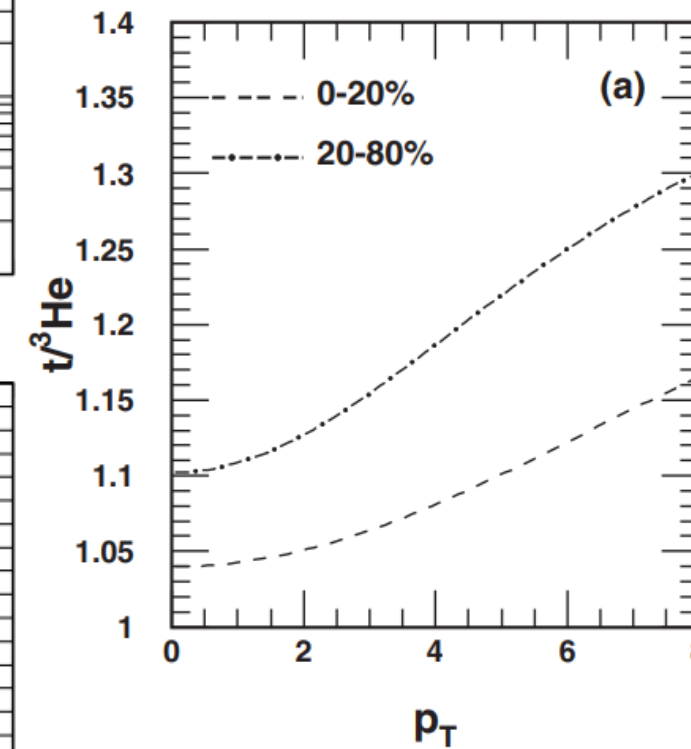
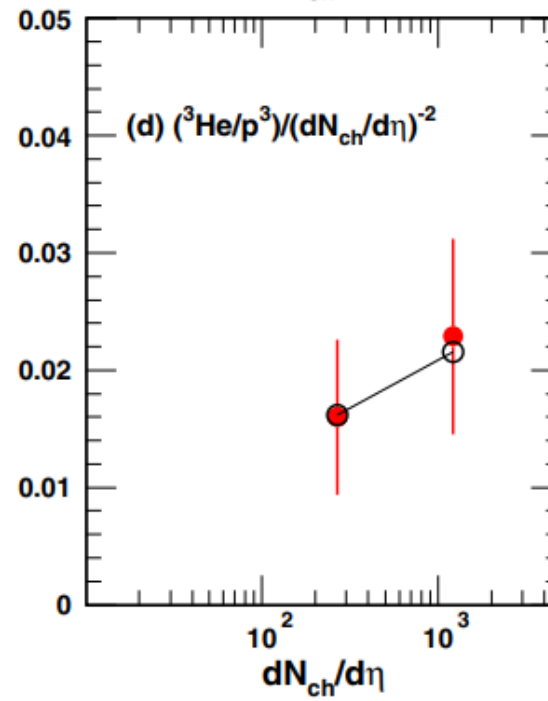
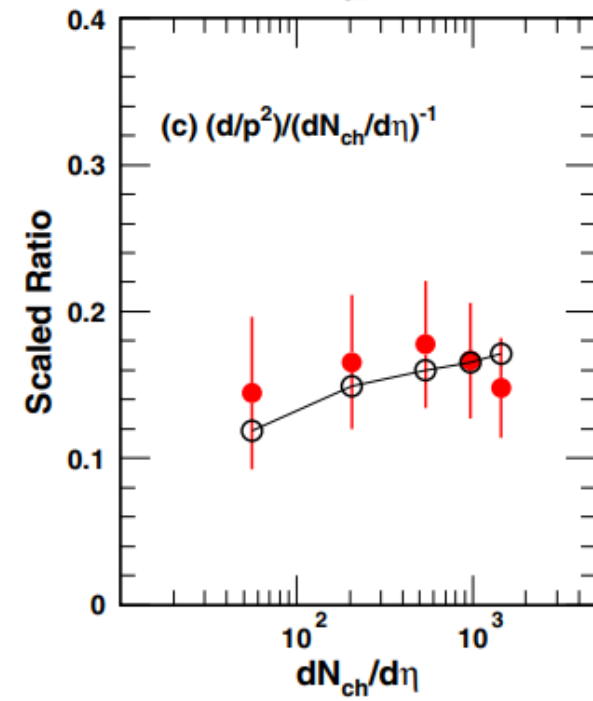
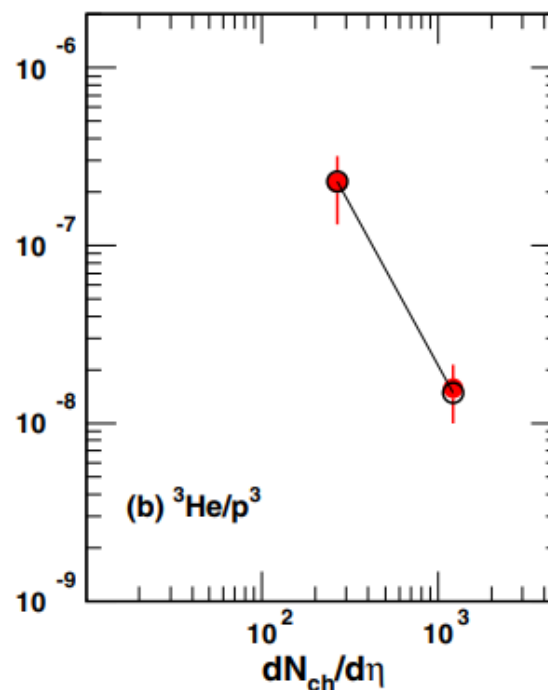
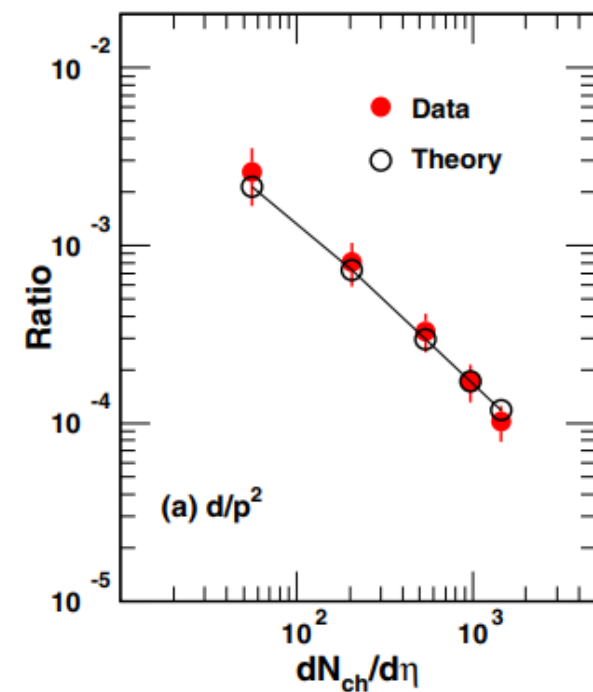
TABLE I. Averaged transverse momenta $\langle p_T \rangle$ and yield rapidity densities dN/dy of d , ^3He , and t in different centralities in Pb-Pb collisions at $\sqrt{s_{NN}} = 2.76$ TeV. Experimental data in the third and fifth columns are from Ref. [18]. Theoretical results are in the fourth and sixth columns.

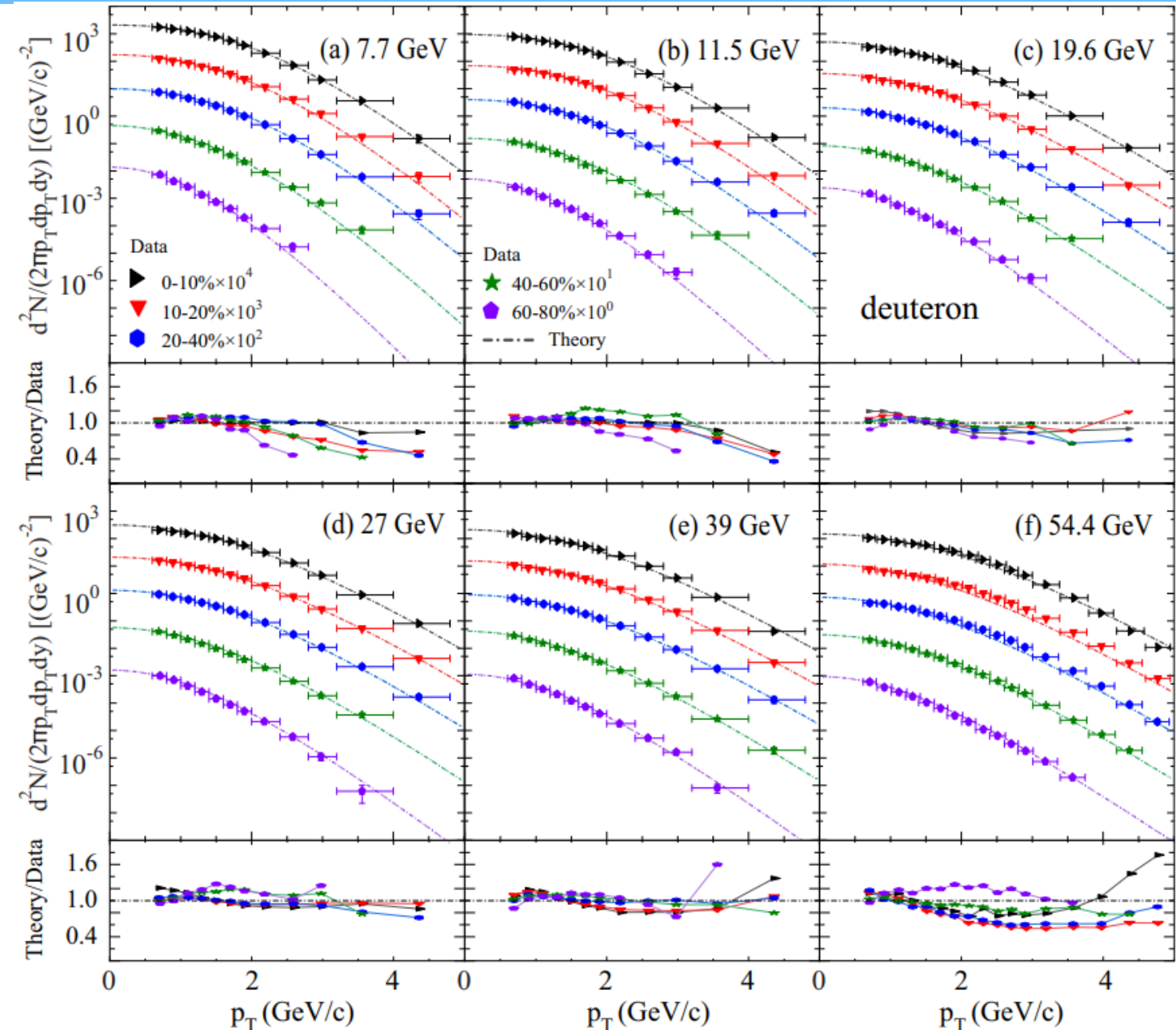
$\langle p_T \rangle$			dN/dy		
Centrality	Data	Theory	Data	Theory	
d	0–10%	$2.12 \pm 0.00 \pm 0.09$	2.19	$(9.82 \pm 0.04 \pm 1.58) \times 10^{-2}$	11.38×10^{-2}
	10–20%	$2.07 \pm 0.01 \pm 0.10$	2.12	$(7.60 \pm 0.04 \pm 1.25) \times 10^{-2}$	7.55×10^{-2}
	20–40%	$1.92 \pm 0.00 \pm 0.11$	1.95	$(4.76 \pm 0.02 \pm 0.82) \times 10^{-2}$	4.28×10^{-2}
	40–60%	$1.63 \pm 0.01 \pm 0.09$	1.62	$(1.90 \pm 0.01 \pm 0.41) \times 10^{-2}$	1.71×10^{-2}
	60–80%	$1.29 \pm 0.01 \pm 0.14$	1.28	$(0.51 \pm 0.01 \pm 0.14) \times 10^{-2}$	0.42×10^{-2}
^3He	0–20%	$2.83 \pm 0.05 \pm 0.45$	2.95	$(2.76 \pm 0.09 \pm 0.62) \times 10^{-4}$	2.60×10^{-4}
	20–80%	$2.65 \pm 0.06 \pm 0.45$	2.18	$(5.09 \pm 0.24 \pm 1.36) \times 10^{-5}$	5.14×10^{-5}
t	0–20%	— — —	2.97	— — —	2.77×10^{-4}
	20–80%	— — —	2.20	— — —	5.84×10^{-5}

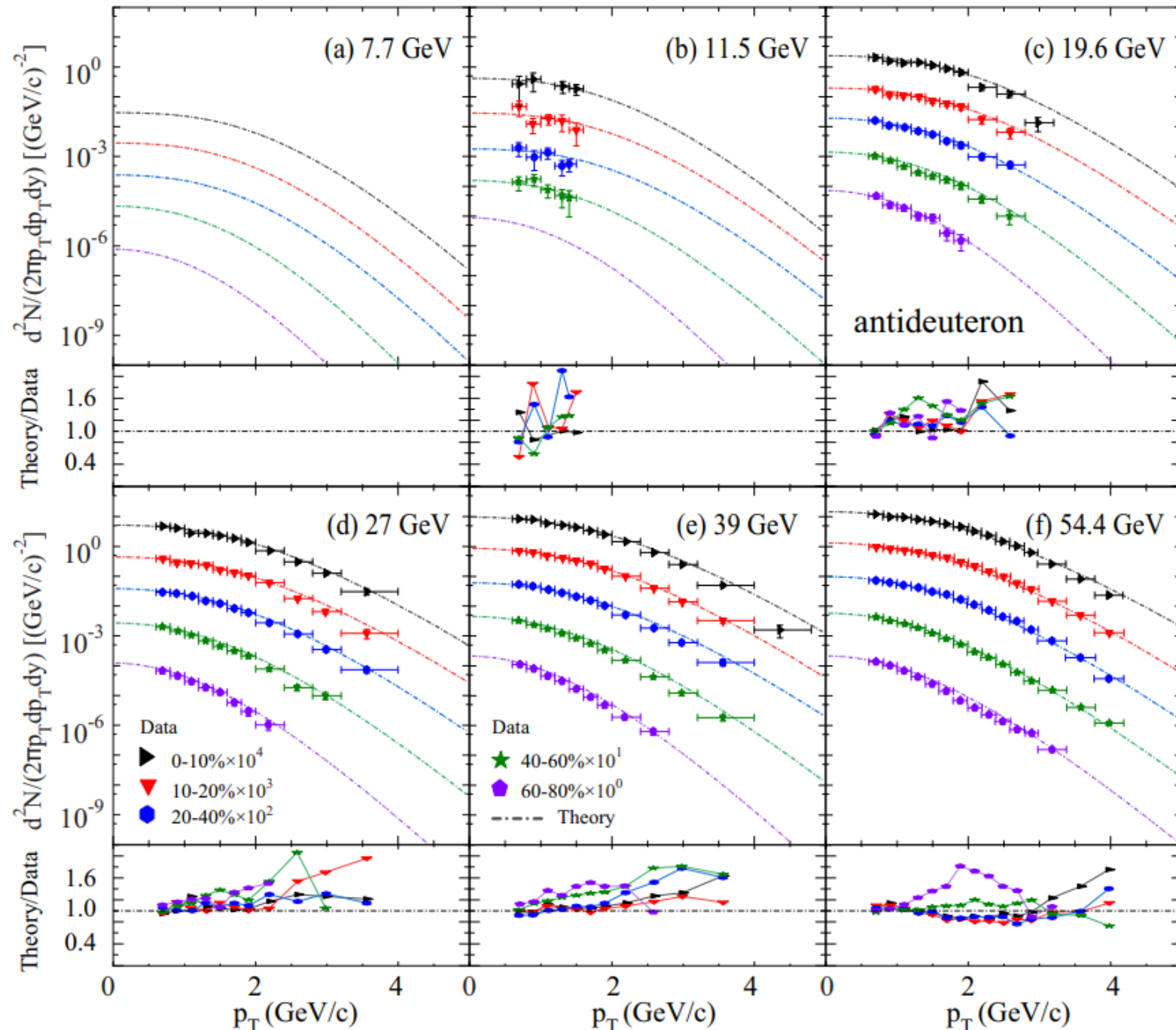
Pb-Pb 2.76 TeV



Pb-Pb 2.76 TeV







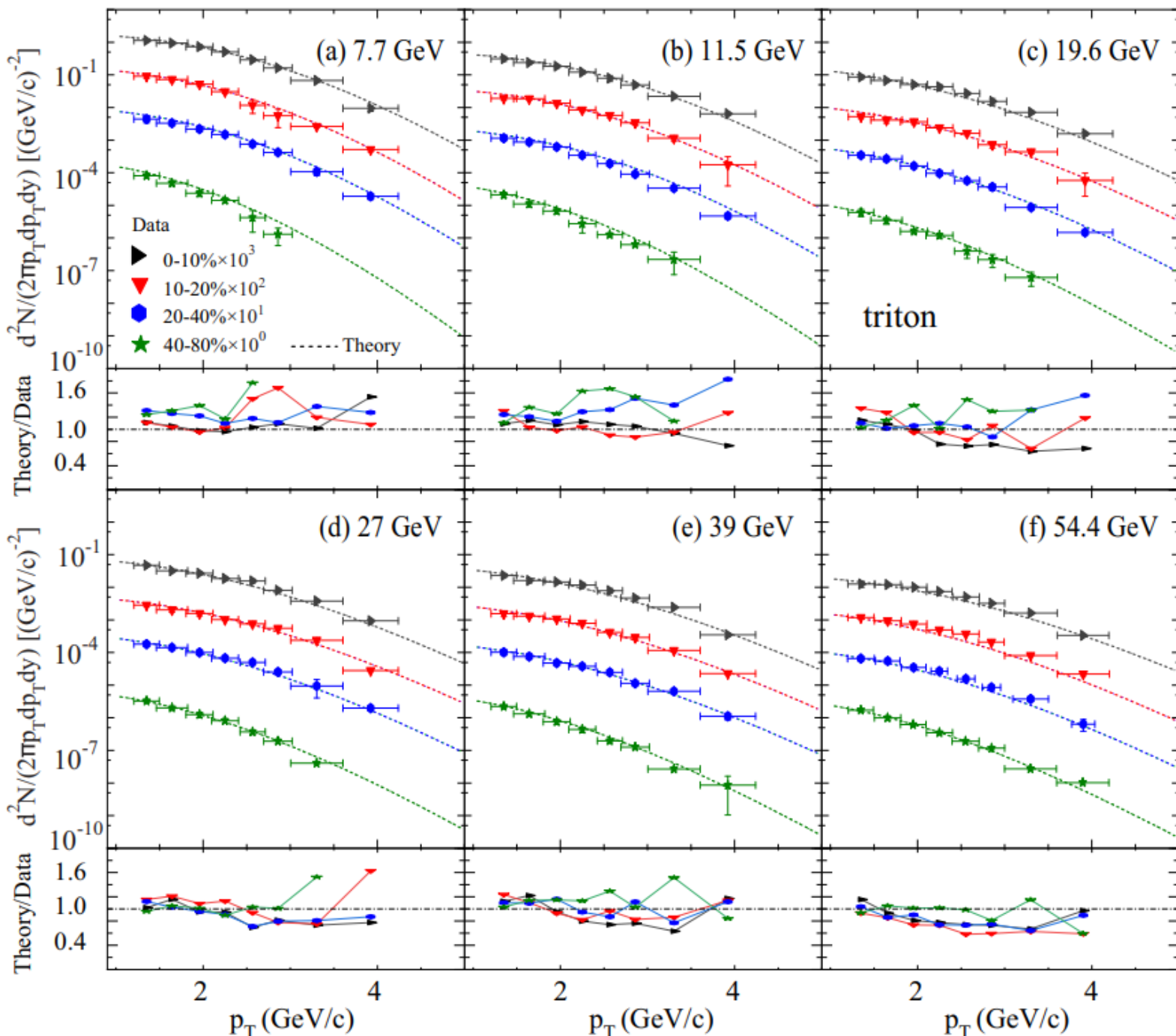
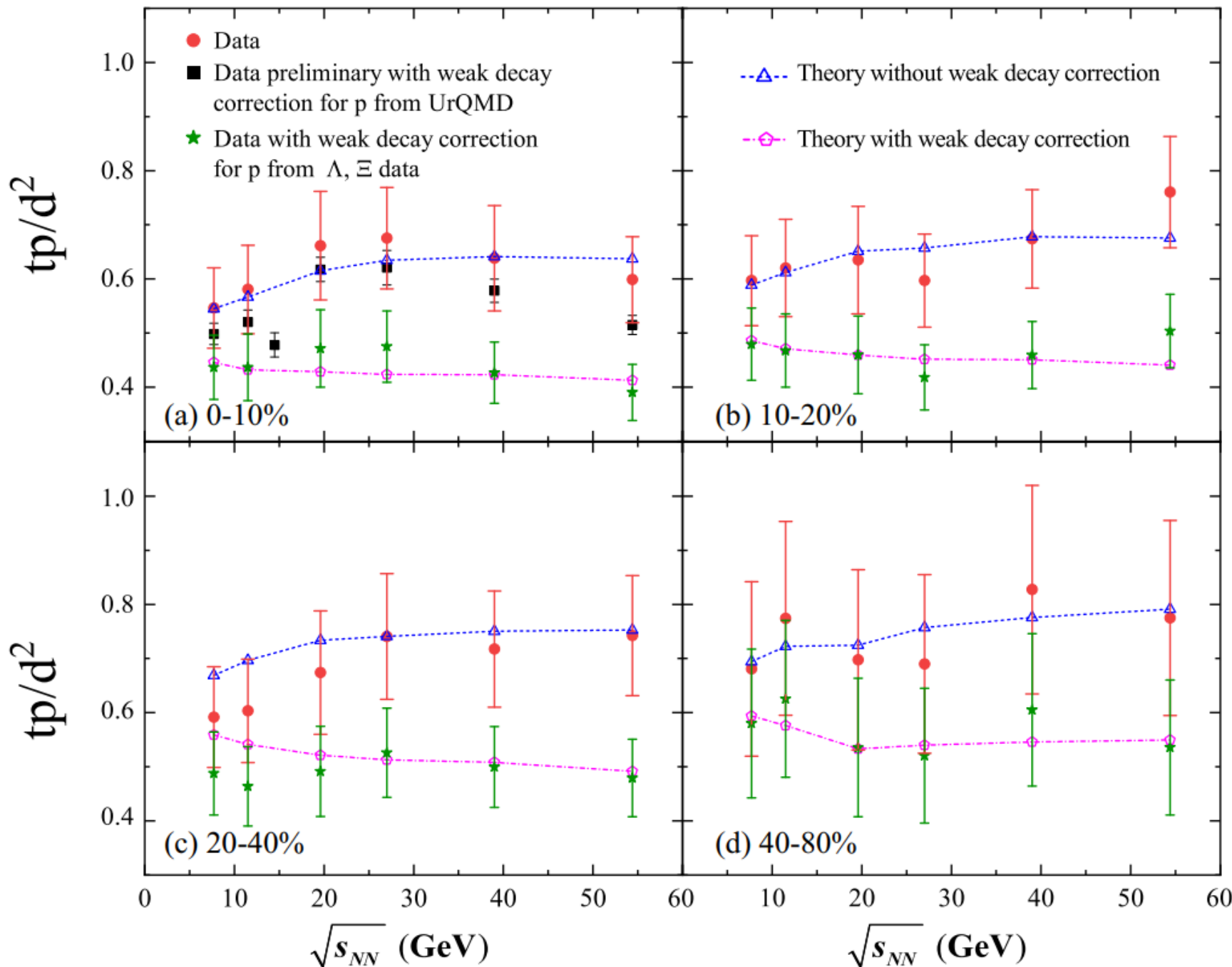


TABLE II. Yield densities dN/dy of d , \bar{d} , t , and \bar{t} at midrapidity in Au-Au collisions in different centralities at $\sqrt{s_{\text{NN}}} = 7.7, 11.5, 19.6, 27, 39, 54.4$ GeV. Data are from Refs. [43,45].

$\sqrt{s_{\text{NN}}}$	Centrality	d		\bar{d}		t		\bar{t}
		data	theory	data	theory	data	theory	theory
7.7 GeV	0–10 %	$140.99 \pm 0.41 \pm 10.97$	142.52	\sim	2.43	21.64	22.06	1.48
	10–20 %	$93.87 \pm 0.32 \pm 7.92$	96.73	\sim	1.94	15.76	16.51	1.41
	20–40 %	$49.06 \pm 0.16 \pm 5.38$	51.86	\sim	1.46	7.30	9.23	1.33
	40–60 %	$15.48 \pm 0.09 \pm 2.92$	16.52	\sim	0.89	1.25	1.44	1.25
	60–80 %	$3.13 \pm 0.05 \pm 0.91$	3.28	\sim	0.22			0.36
		$\times 10^{-2}$	$\times 10^{-2}$	$\times 10^{-4}$	$\times 10^{-4}$	$\times 10^{-3}$	$\times 10^{-3}$	$\times 10^{-9}$
	0–10 %	$63.05 \pm 0.14 \pm 4.55$	65.11	$3.29 \pm 0.63 \pm 1.10$	3.21	5.83	6.07	6.50
	10–20 %	$41.02 \pm 0.11 \pm 3.39$	42.46	$1.92 \pm 0.32 \pm 0.57$	2.31	4.00	4.23	4.94
	20–40 %	$21.92 \pm 0.06 \pm 2.23$	22.32	$1.05 \pm 0.17 \pm 0.34$	1.42	1.96	2.34	3.28
	40–60 %	$6.73 \pm 0.03 \pm 1.17$	6.96	\sim	0.84	0.34	0.34	3.01
11.5 GeV	60–80 %	$1.31 \pm 0.02 \pm 0.40$	1.38	\sim	0.29			1.48
		$\times 10^{-2}$	$\times 10^{-2}$	$\times 10^{-4}$	$\times 10^{-4}$	$\times 10^{-4}$	$\times 10^{-4}$	$\times 10^{-7}$
	0–10 %	$27.45 \pm 0.06 \pm 2.04$	29.12	$17.88 \pm 0.52 \pm 3.14$	20.45	15.70	16.43	8.33
	10–20 %	$18.78 \pm 0.05 \pm 1.57$	20.09	$13.16 \pm 0.45 \pm 2.36$	15.38	10.20	11.98	6.92
	20–40 %	$9.73 \pm 0.03 \pm 1.00$	10.05	$10.33 \pm 0.27 \pm 1.87$	11.44	5.37	6.23	6.73
	40–60 %	$3.20 \pm 0.01 \pm 0.55$	3.30	$5.48 \pm 0.20 \pm 1.15$	6.65	0.90	0.95	6.10
	60–80 %	$0.68 \pm 0.007 \pm 0.21$	0.67	$2.07 \pm 0.14 \pm 0.70$	2.23			2.80
		$\times 10^{-2}$	$\times 10^{-2}$	$\times 10^{-4}$	$\times 10^{-4}$	$\times 10^{-4}$	$\times 10^{-4}$	$\times 10^{-6}$
	0–10 %	$18.44 \pm 0.04 \pm 1.28$	19.57	$41.35 \pm 0.54 \pm 4.63$	44.34	7.98	8.35	2.59
	10–20 %	$12.83 \pm 0.03 \pm 1.05$	12.98	$32.35 \pm 0.47 \pm 3.85$	35.17	5.07	5.71	2.35
27 GeV	20–40 %	$6.84 \pm 0.01 \pm 0.70$	7.05	$23.03 \pm 0.28 \pm 2.79$	24.68	3.17	3.38	2.09
	40–60 %	$2.33 \pm 0.009 \pm 0.43$	2.45	$11.48 \pm 0.21 \pm 2.45$	12.92	0.49	0.59	1.55
	60–80 %	$0.49 \pm 0.004 \pm 0.17$	0.52	$3.33 \pm 0.11 \pm 1.23$	3.87			0.60
		$\times 10^{-2}$	$\times 10^{-2}$	$\times 10^{-4}$	$\times 10^{-4}$	$\times 10^{-4}$	$\times 10^{-4}$	$\times 10^{-6}$
	0–10 %	$12.73 \pm 0.02 \pm 0.95$	13.27	$79.96 \pm 0.46 \pm 6.35$	85.57	4.21	4.59	6.60
	10–20 %	$8.78 \pm 0.01 \pm 0.69$	9.20	$62.39 \pm 0.40 \pm 4.60$	64.75	3.01	3.32	5.80
	20–40 %	$4.81 \pm 0.008 \pm 0.48$	5.03	$41.24 \pm 0.23 \pm 4.11$	42.81	1.68	1.92	4.46
	40–60 %	$1.72 \pm 0.004 \pm 0.30$	1.82	$19.24 \pm 0.15 \pm 3.26$	22.45	0.36	0.37	3.33
	60–80 %	$0.37 \pm 0.002 \pm 0.12$	0.37	$5.50 \pm 0.09 \pm 1.80$	6.77			1.33
		$\times 10^{-2}$	$\times 10^{-2}$	$\times 10^{-2}$	$\times 10^{-2}$	$\times 10^{-4}$	$\times 10^{-4}$	$\times 10^{-5}$
54.4 GeV	0–10 %	10.28	9.58	1.21	1.26	2.67	2.47	1.22
	10–20 %	7.07	7.15	0.93	0.93	2.36	2.14	0.94
	20–40 %	3.89	3.67	0.57	0.59	1.29	1.16	0.69
	40–60 %	1.40	1.27	0.28	0.28	0.25	0.21	0.39
	60–80 %	0.31	0.28	0.07	0.08			0.13



We find:

- Data for p_T spectra, averaged p_T , yield rapidity densities, yield ratios, especially for their interesting behaviors as functions of the collision energy and the collision centrality, can be well reproduced.
- Predictions of $t/{}^3\text{He}$ can further reveal production mechanisms of light nuclei.

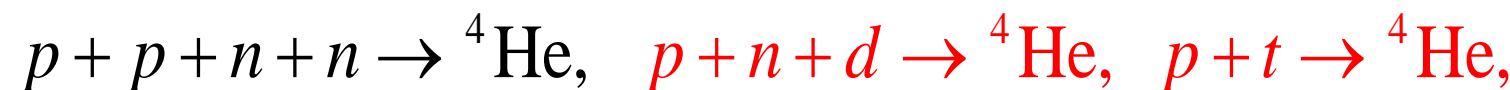
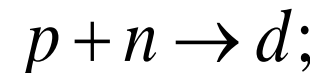
IV. Summary

- ◆ We developed an analytical coalescence model to deal with productions of different light nuclei in relativistic heavy-ion collisions.
- ◆ The relationships of light nuclei with primordial nucleons and effects of different factors (e.g., the whole hadronic system scale, the sizes of the formed light nuclei) on light nuclei production were clearly given.
- ◆ We applied the analytical coalescence model to heavy ion collisions at RHIC and LHC to successfully explain the experimental measurements.
- ◆ We found the coalescence mechanism worked well in describing light nuclei production in a wide collision energy range from 3 GeV to 5.02 TeV.

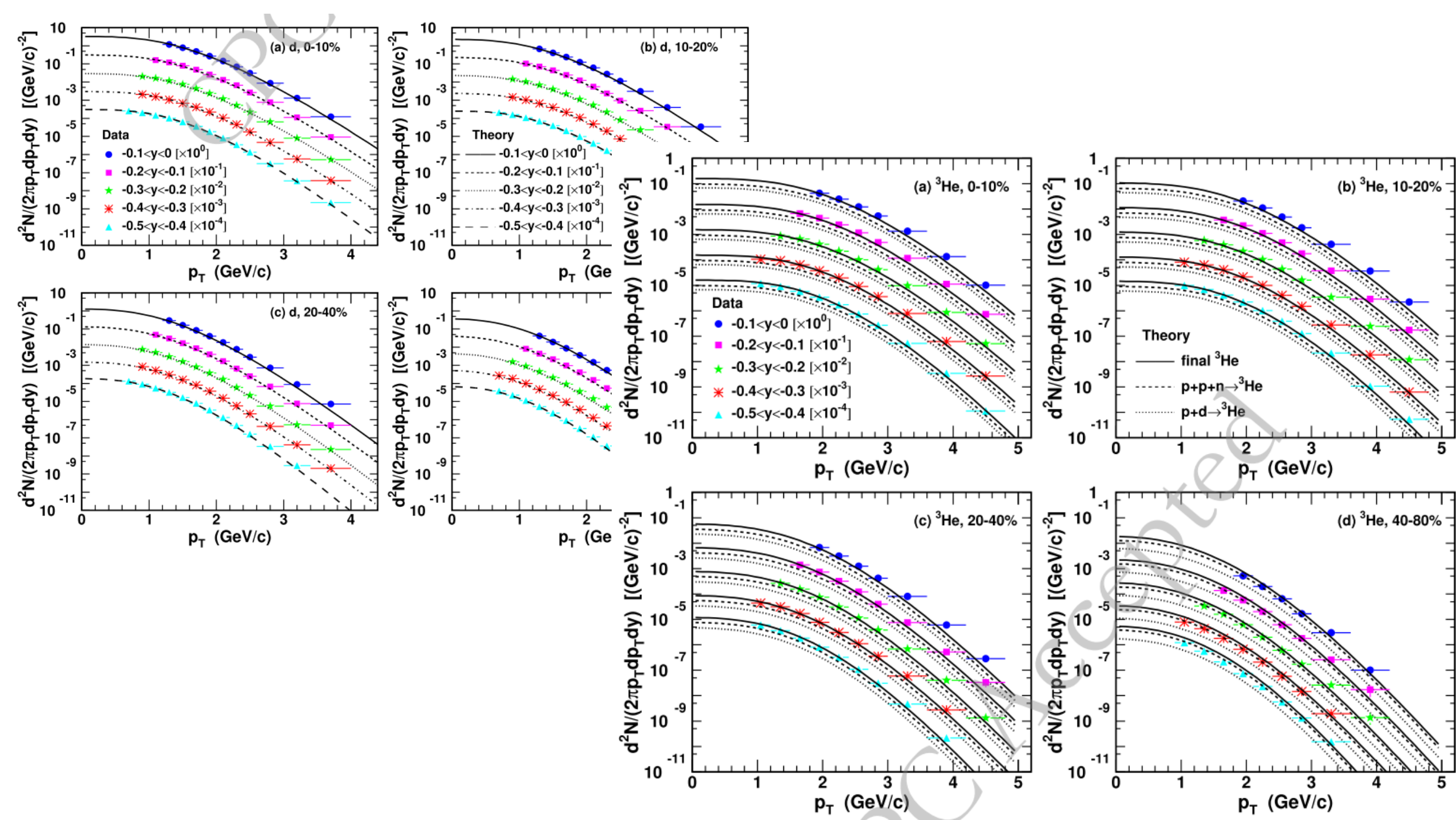
Thank you !

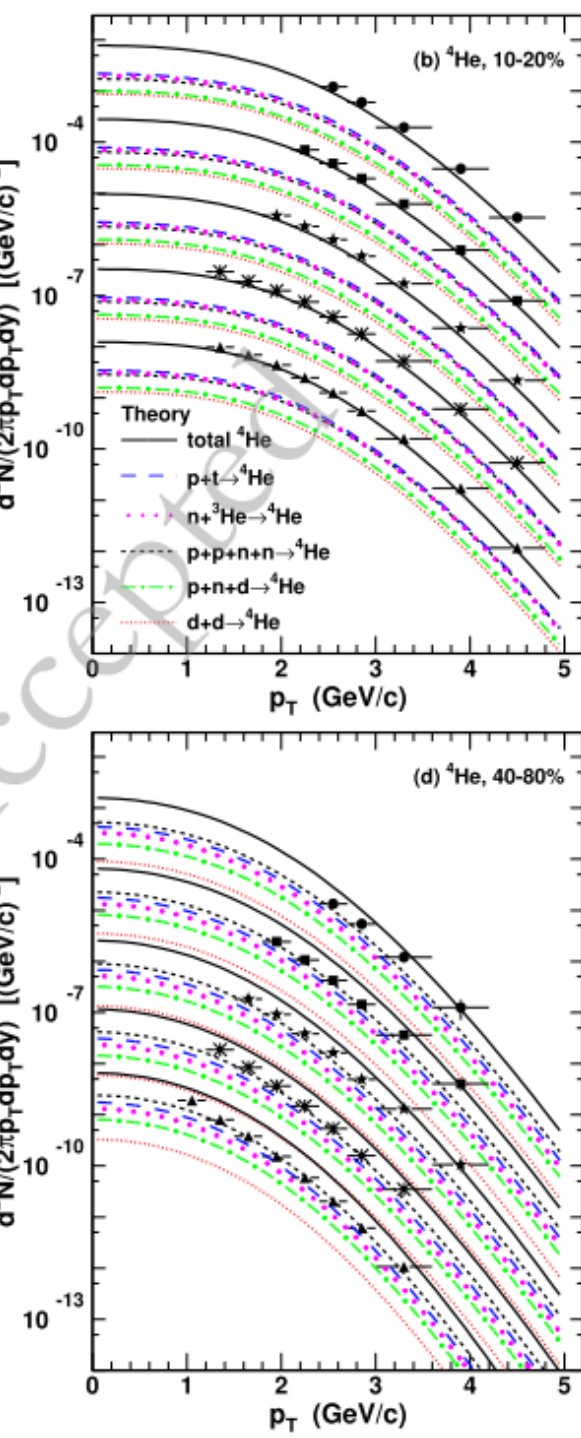
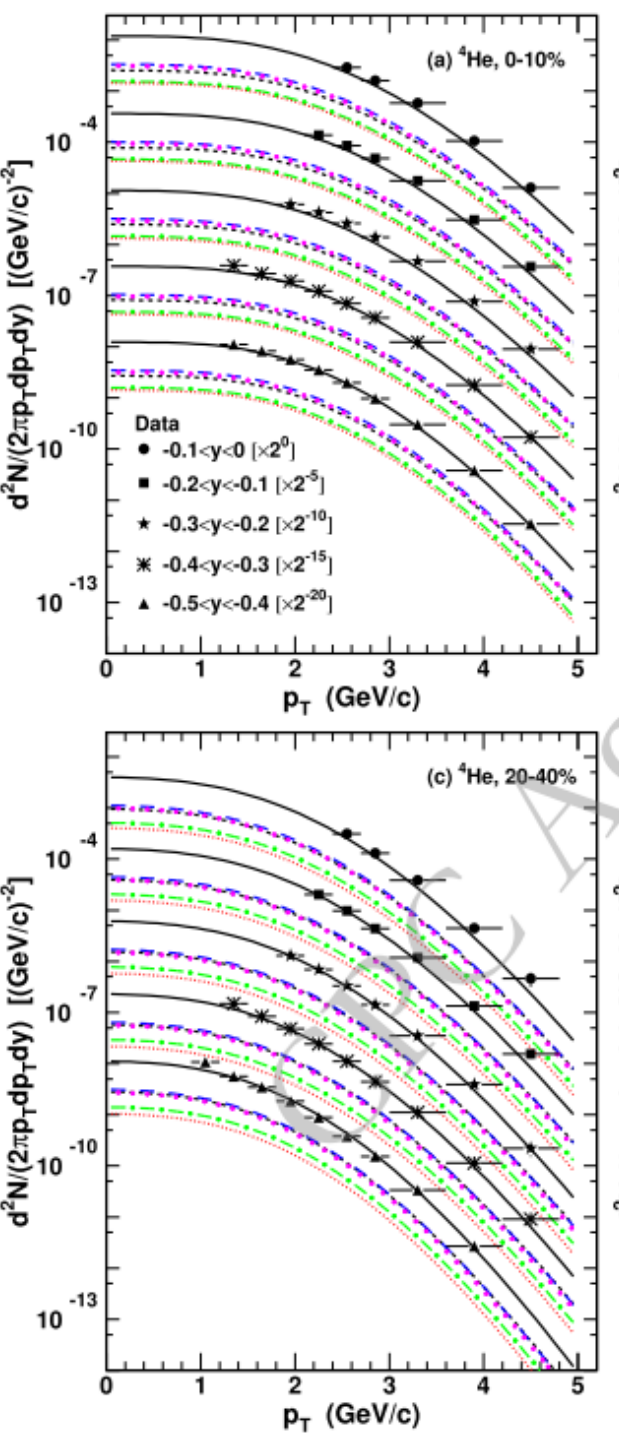
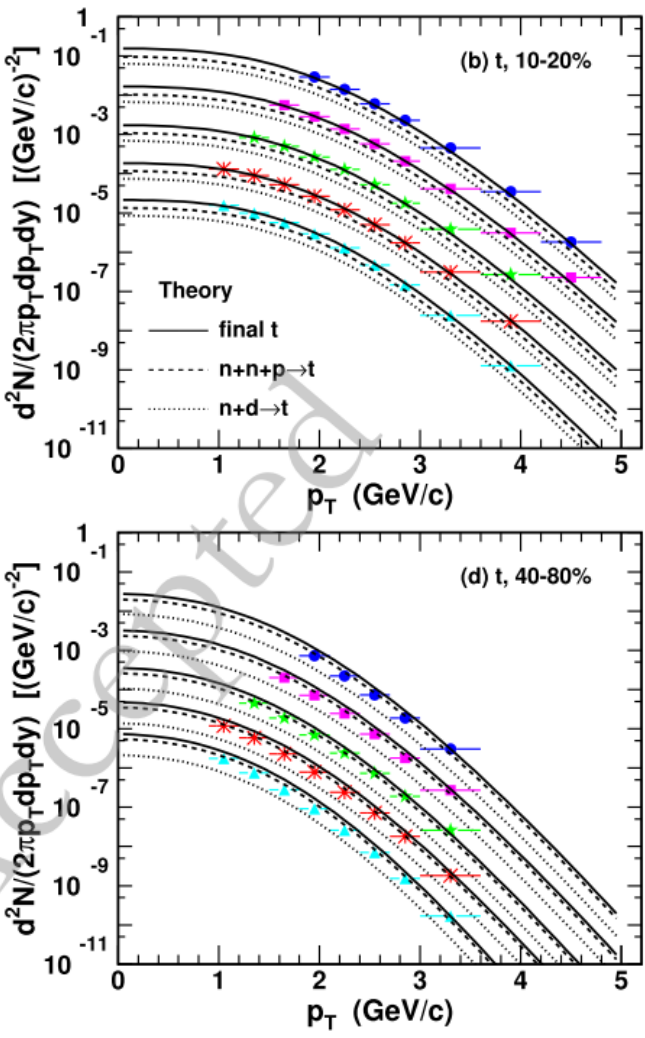
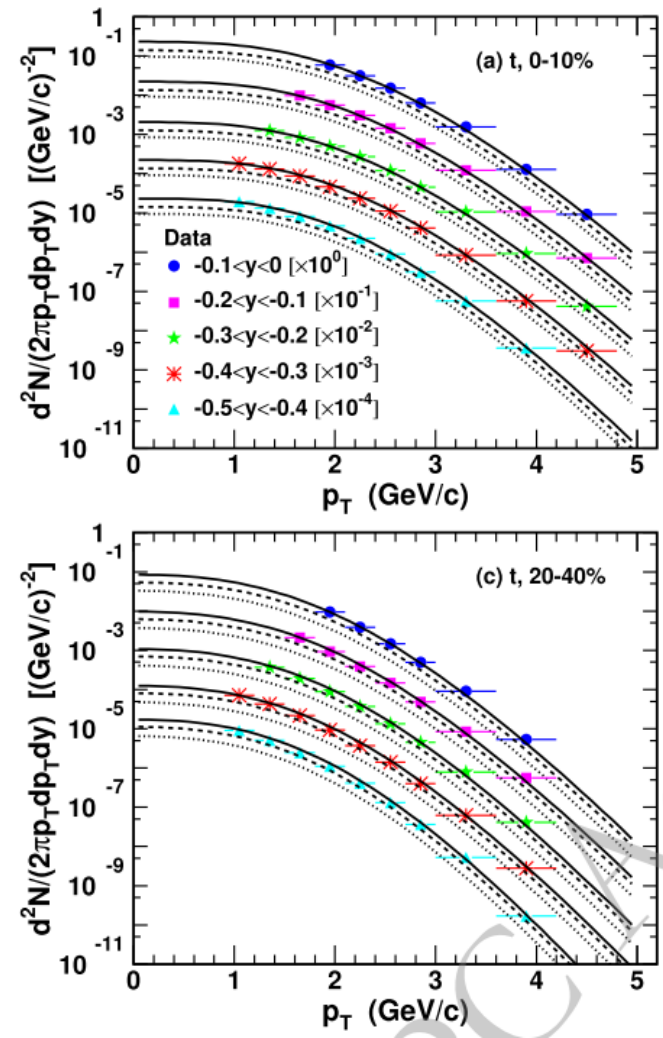
Extended applications

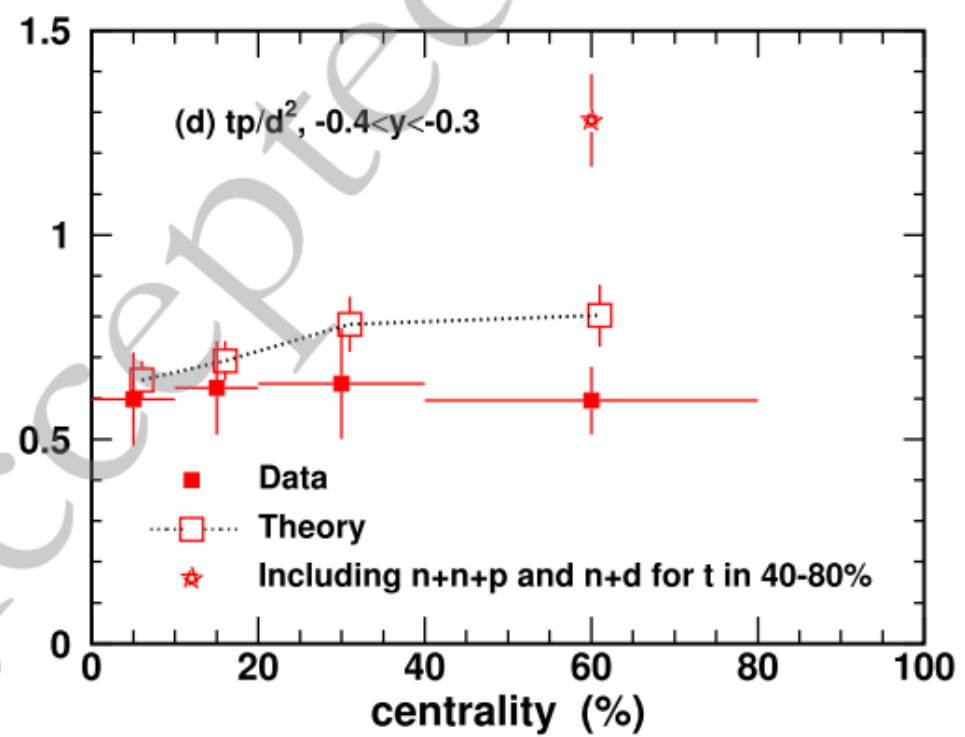
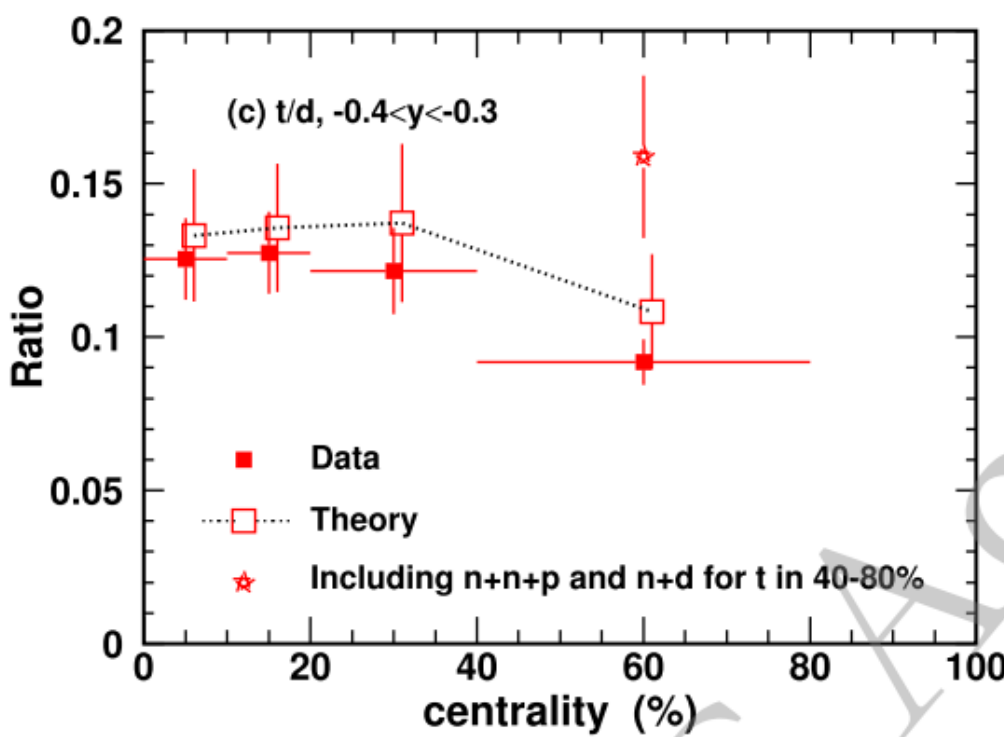
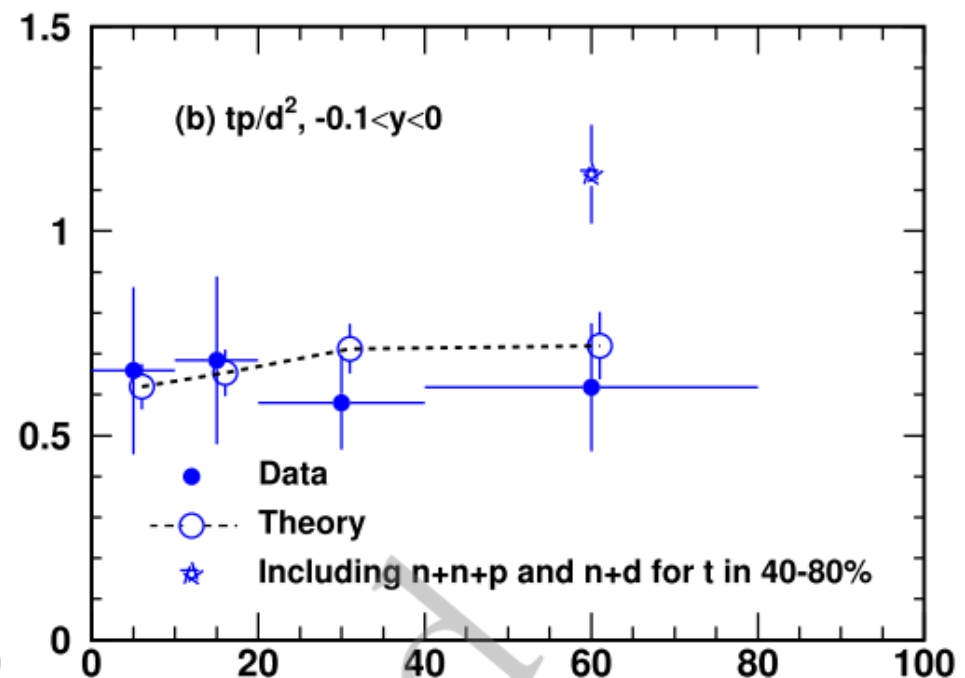
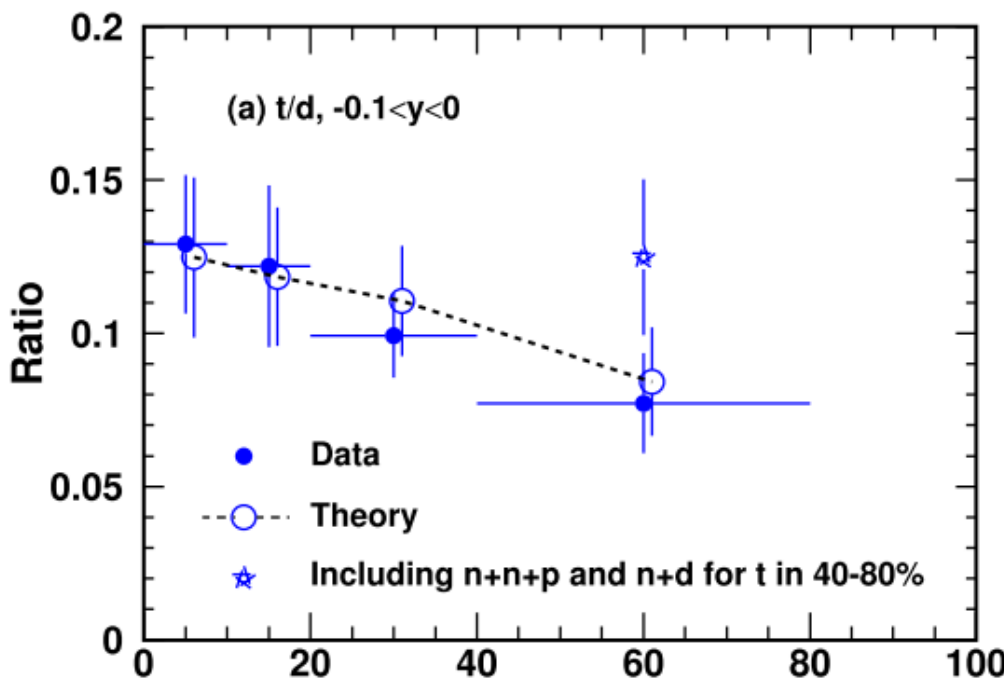
Au-Au collisions at $\sqrt{s_{NN}} = 3 \text{ GeV}$, consider other coalescence sources



RQW, J.P. Lv, Y.H. Li, J. Song, F.L. Shao, Chin. Phys. C 48 053112 (2024).







Extended applications

Hyper triton, heavy flavor molecular states...

